

2010

PROTEOMIC ANALYSIS OF REDOX SENSITIVE PROTEINS IN A HUNTINGTON'S DISEASE CELL MODEL

Andrea L. Pitts

Follow this and additional works at: <https://ir.lib.uwo.ca/digitizedtheses>

Recommended Citation

Pitts, Andrea L., "PROTEOMIC ANALYSIS OF REDOX SENSITIVE PROTEINS IN A HUNTINGTON'S DISEASE CELL MODEL" (2010). *Digitized Theses*. 4887.
<https://ir.lib.uwo.ca/digitizedtheses/4887>

This Thesis is brought to you for free and open access by the Digitized Special Collections at Scholarship@Western. It has been accepted for inclusion in Digitized Theses by an authorized administrator of Scholarship@Western. For more information, please contact wlsadmin@uwo.ca.

PROTEOMIC ANALYSIS OF REDOX SENSITIVE
PROTEINS IN A HUNTINGTON'S DISEASE CELL
MODEL

(Spine Title: Proteomic Analysis of Huntington's Disease)

(Thesis Format: Monograph)

by

Andrea L. Pitts

Graduate Program in Biology

Submitted in partial fulfillment of the
requirements for the degree of
Master of Science

School of Graduate and Postdoctoral Studies

The University of Western Ontario

London, Ontario, Canada

May 2010

© Andrea L. Pitts 2010

School of Graduate and Postdoctoral Studies

CERTIFICATE OF EXAMINATION

Supervisor

Dr. Robert Cumming

Examiners

Dr. Sashko Damjanovski

Advisors

Dr. Sashko Damjanovski

Dr. Ron Podesta

Dr. Paul Walton

Dr. Charles Trick

The thesis by

Andrea L Pitts

Entitled:

**Proteomic Analysis of Redox Sensitive Proteins in a
Huntington's Disease Cell Model**

is accepted in partial fulfillment of the

requirements for the degree of

Master of Science

Date

Chair of the Thesis Examination Board

TABLE OF CONTENTS

CERTIFICATE OF EXAMINATION.....	II
ABSTRACT.....	III
ACKNOWLEDGEMENTS.....	IV
TABLE OF CONTENTS.....	V
LIST OF TABLES.....	VIII
LIST OF FIGURES.....	IX
LIST OF APPENDICES.....	X
LIST OF ABBREVIATIONS.....	XI
1. Introduction	
1.1 Problem Statement.....	1
1.2 HD Characterization and Wild-type Protein Function....	2
1.3 Hallmarks of HD Pathology	
1.3.1 Aggregate formation.....	4
1.3.2 Transcriptional deregulation.....	6
1.3.3 Perturbed mitochondrial function.....	7
1.3.4 Oxidative stress.....	8
1.4 Proposed mechanism for HD neuronal toxicity.....	9
1.5 Current HD treatments.....	10
1.6 Hypothesis and investigative plan.....	11
2. Materials and Methods	
2.1 Cell culture and transgene induction.....	13
2.2 Determination of mitochondrial produced ROS.....	14
2.3 Cell fractionation and protein lysate preparation.....	14

2.4	Cell lysate protein content.....	15
2.5	Two-dimension Redox PAGE.....	15
2.5.1	Positive and negative controls.....	15
2.6	DSB visualization.....	16
2.7	Identification of redox sensitive proteins.....	16
2.8	Immunoblot analysis.....	17
2.9	MTT and trypan blue cell viability assays.....	18
2.10	Analysis of DMP specific changes in the PC12 disulfide proteome.....	18
3.	Results	
3.1	mHtt ^{103Q} and mitochondrial produced ROS in PC12 cells.....	20
3.2	Analysis of changes in the PC12 disulfide proteome specific to mHtt ^{103Q} expression.....	23
3.3	Identification of proteins that undergo changes in DSBF specific to mHtt ^{103Q} expression.....	30
3.4	Verification of mHtt ^{103Q} induced Prx-1 diminishment..	30
3.5	The effects of thiol-based compounds on PC12 cell viability after mHtt ^{103Q} induction.....	31
3.6	The effects of 0.1 mM DMP in mHtt ^{103Q} induced Prx-1 diminishment.....	34
3.7	Verification of the effects of DMP on Prx-1.....	41
4.	Discussion	
4.1	Overview.....	44
4.2	mHtt ^{103Q} expression increases mitochondrial	

	produced ROS.....	44
4.3	A mHtt ^{103Q} induced increase in mitochondrial ROS production is correlated with aberrant DSBF of key intracellular antioxidant proteins.....	45
4.4	DMP and BME increase cell viability in HD PC12 cell model.....	48
4.5	DMP preserves the homodimeric and monomeric Forms of Prx-1.....	51
4.6	Conclusions and Future Directions.....	52
	Bibliography.....	57
	Appendix.....	62

LIST OF TABLES

Table 1	Summary of disulfide bonded proteins identified with MALDI- <i>tof</i>	29
----------------	--	----

LIST OF FIGURES

Figure 1	Effect of PC12 mHtt ^{103Q} induction on mitochondrial produced reactive oxygen species.....	22
Figure 2	Separation of disulfide bonded proteins from the soluble Triton-X100 fraction by 2D Redox PAGE.....	25
Figure 3	Negative and positive controls for 2D Redox PAGE.....	27
Figure 4	Timecourse analysis of disulfide bond formation of Peroxiredoxin-1 through one-dimensional nonreducing and reducing SDS-PAGE followed by immunoblotting.....	33
Figure 5	Growth of mHtt induced PC12 cells in the presence of various concentrations of penacillamine, BME, cystamine and DMP.....	36
Figure 6	Trypan Blue confirmation of induced PC12 cell growth in the presence of 0.1 μ M penacillamine, BME, cystamine and DMP.....	38
Figure 7	The effect of 0.1 μ M DMP on Prx-1 disulfide bond formation by 2D Redox PAGE.....	40
Figure 8	Timecourse analysis of Peroxiredoxin-1 disulfide bond formation in the presence of 0.1 μ M DMP with one-dimensional nonreducing and reducing SDS-PAGE followed by immunoblotting.....	43
Figure 9	Proposed model of mHtt-mediated effects on protein disulfide bond formation.....	54

LIST OF APPENDICES

Appendix 1

Supplementary Figure 1	Cell Model: Transgenic PC12 Cell Line.....	64
Supplementary Figure 2	Schematic Explanation of Two-dimensional Redox PAGE.....	66
Supplementary Figure 3	Prx-1 Structure and Catalytic Function Under Oxidative Stress.....	68

LIST OF ABBREVIATIONS

%	Percent
°C	Degree Celsius
ASK-1	Apoptosis signaling kinase factor- 1
ATP	Adenosine triphosphate
BME	Beta-mercaptoethanol
BSA	Bovine serum albumin
CAG	Cysteine, Adenine, Guanine
CBP	CREB binding protein
CHCA	α -Cyano-4-hydroxycinnamic acid
CNS	Central nervous system
CO ₂	Carbon dioxide
CoQ10	Coenzyme Q-10
CREB	Cyclic-adenosine monophosphate response element binding protein
Cys-SH	Cysteine sulfhydryl
DMEM	Dubecco's modified Egel's media
DMP	Dimercaptopropanol
DMSO	Dimethylsulfoxide
DNA	Deoxyribonucleic acid
DRPLA	Dentatorubralpallodolusian
DSBF	Disulfide bond formation
DTT	Dithiothreitol
ECL	Enhanced chemiluminescence
ETC	Electron transport chain

G	Gravitational constant ($6.67 \times 10^{-11} \text{ m}^3/\text{kg}/\text{s}^2$)
GFP	Green fluorescence protein
GRx	Glutaredoxin
GSH	Glutathione
HD	Huntington's disease
H ₂ O ₂	Hydrogen peroxide
HSP	Heat shock protein
HTT	Huntington gene
Hz	Hertz
IA	Iodoacetamide
kDa	Kilo Dalton
MALDI	Matrix-assisted laser desorption/ ionization
mA	Milliampere
min	Minute
mHtt	Mutant Huntington protein
mM	Millimolar
mRNA	Messenger Ribonucleic acid
MTT	3-(4,5-Dimethylthiazol-2-yl)-2,5-diphenyltetrazolium bromide
NAC	N-acetylcysteine
Nd:YAG	neodymium-doped yttrium aluminum garnet
nm	Nanometers
3-NP	3- Nitropropionic acid
PAGE	Polyacrylamide gel electrophoresis
PBS	Phosphate buffered saline
PC12	Pheochromocytoma clone-12

PMSF	Phenylmethansulfonylfluoride
PolyQ	Polygluatmine
ppm	Parts per million
Prx	Peroxiredoxin
ROS	Reactive oxygen species
SBMA	Spinobulbar muscular atrophy
SCA	Spinocerebellar ataxia
SDS	Sodium dodecyl sulphate
SOD	Superoxide dismutase
TBP	TATA binding protein
TBST	Tris-buffered saline
TFA	Trifluoroacetic acid
Trx	Thioredoxin

Chapter 1

Introduction

1.1 Problem statement

In 1993, the causative gene (*HTT*) of Huntington's disease (HD) was identified and research extensively began on the disease (Gil and Rego. 2008). The discovery of *HTT* gave rise to expectations that the mechanisms underlying disease progression would soon be discovered and treatments to prevent disease onset or slow progression would ensue. However, seventeen years later, HD etiology still remains poorly understood (Stack, et al. 2008). While many altered cellular processes have been linked to mutations in the *HTT* gene, a mechanistic understanding of how these changes contribute to HD progression is not well elucidated. One of the most well characterized cellular aberrations associated with HD and neurodegenerative diseases alike is oxidative stress (Trushina and McMurray. 2007). Widespread oxidative damage is well documented with HD progression and a range of antioxidant therapies have shown promising neuroprotection in *in vitro* and *in vivo* models (Aiken, et al. 2004, Schilling, et al. 2001). Mechanistically how an oxidative stress situation is allowed to progress or how antioxidant compounds exert their protective effects in HD remains unknown. The purpose of this thesis was to (1) determine whether a mutant Huntingtin (mHtt) induced change in the oxidative status of a PC12 nerve cell model may contribute via aberrant disulfide bond formation (DSBF) to HD neuronal toxicity and (2) resolve whether or not

thiol-based compounds counter the neuronal toxicity via inhibition of mHtt induced changes in DSBF.

1.2 HD characterization and wild-type protein function

HD is a progressive neurodegenerative disease, whose clinical manifestations and pattern of inheritance was first described in the 19th century by a physician, George Huntington (Jenkins and Conneally, 1989). Clinically, HD occurs across all ethnicities and spans all age groups, from 2 to 80 years of age (Gil and Rego. 2008). Most commonly however, HD occurs in mid-life with the selective loss of the striatum and cerebral neurons in the brain with late stage neurodegeneration also observed in the hippocampus and hypothalamus (Vonsattel and DiFiglia, 1998, Li and Li. 2004). The first signs of HD are subtle, awkward movements and clumsiness collectively known as chorea, that lead to more uncoordinated movements as the disease progresses. Over time, HD results in a devastating loss of voluntary movement, cognitive and psychiatric disturbances producing dementia and invariably leads to death approximately 10-15 years after disease onset (Sorolla, et al. 2008). HD belongs to a family of eight polyglutamine (polyQ) neurodegenerative disorders which include dentatorubralpallodolusian atrophy (DRPLA), spinobulbar muscular atrophy (SBMA) and spinocerebellar ataxia (SCA) types 1-3, 6, 7, and 17 (Li and Li. 2004). Specifically, HD is the most common polyQ disorder, affecting 3-10 subjects per 100,000 people in North America and Western Europe (Gil and Rego. 2008).

The Huntington Gene (*HTT*) is located on the short arm of chromosome 4 and is inherited in an autosomal dominant manner with the expansion of a DNA trinucleotide

repeat (CAG) near the 5' end in exon 1 of the HTT gene coding sequence (Sorolla, et al. 2008). The length of the polyglutamine expansion in HD is a major determinant of disease severity, age of onset and results in the formation of a large aggregated form of the protein that cannot function properly within the cell (DiFiglia, et al. 1997). It has been well documented that Htt contains anywhere from 11 to 34 polyglutamine repeats in affected individuals (Gil and Rego. 2008, Li and Li. 2004). However, 35 polyglutamine repeats is essentially the threshold for HD manifestation with increasingly severe phenotypes arising as the length of the polyglutamine expansion increases (Schaffar et al., 2004). Thus, HD severity is directly proportional to the length of the polyglutamine expansion. However, age of onset is inversely proportional to the length of polyglutamine expansion as the greater number of repeats, the earlier the age a patient will become symptomatic (Schaffar et al. 2004). Adult onset HD is most commonly associated with 40-50 glutamine repeats whereas lengthier repeats (upwards of 100) result in juvenile and infantile cases (Gil and Rego. 2008). Despite HD's predictable onset, how it progresses mechanistically and even the exact function of the wildtype huntingtin (Htt) protein remains poorly understood.

Htt is a 348 kDa protein (approximately, based on the average number of glutamine residues) composed of >3100 amino acids (Schaffar, et al. 2004). Htt's ubiquitous expression throughout all tissues in the body and subcellular association with the nucleus, endoplasmic reticulum, mitochondria, golgi, and synaptic vesicles have made the identification of it's native and subsequent mutant function difficult (Gutekunst, et al. 1998). Early embryonic studies of gene-targeted mouse models revealed that deletion of the mouse ortholog of the HD gene results in an embryonic lethality (Nasir, et

al. 1995). Interestingly, a subsequent study showed that this embryonic lethality can be rescued with the expression of mutant human Htt, suggesting that the functional role of the Htt protein is independent of polyglutamine length and indicates that the protein acquires a toxic gain of function in mid life (Dragatsis, et al. 1998). Also, several of studies have focused on identifying Htt binding proteins to elucidate it's native role within the cell (Li and Li. 2004). In particular, Htt has been shown to bind to a host of intracellular proteins involved in transcription, trafficking, endocytosis, signaling and metabolism (Li and Li. 2004). The identification of Htt binding proteins coupled with the elucidation of cellular dysfunction associated with mHtt expression has also given valuable insight into the disruption of several intracellular processes and numerous pathological effects specific to HD.

1.3 Hallmarks of HD pathology

1.3.1 Aggregate formation

Aside from the classic neurodegeneration or neuronal toxicity observed in HD, the formation of intracellular aggregates is one of the most prominent microscopic hallmarks of HD and other neurodegenerative polyglutamine diseases alike (DiFiglia, et al. 1997). The expression of mHtt in various cell types results in an irregular distribution of the mutant protein into insoluble cytosolic and nuclear aggregates (DiFiglia, et al. 1997). Mechanistically how mHtt accumulates and forms intracellular aggregates is not entirely known. Even the pathology associated with aggregate formation is not well elucidated. However, two different models known as the Polar Zipper model and the

Transglutaminase model have attempted to provide a mechanism for the aggregate and inclusion body formation seen in Huntington's disease.

According to the Polar Zipper model, the normal tertiary conformation of the Huntingtin protein is destabilized by the presence of an expanded polyglutamine tract resulting in abnormal protein-protein interactions (Hoffner, et al. 2007). Early in vitro evidence showed that exon 1 of the Huntingtin gene promoted aggregate formation with polyQ lengths exceeding 50; however shorter expansions did not promote aggregate formation (Hoffner, et al. 2007). Subsequent analysis revealed the formation of insoluble β -pleated sheets that form polar zipper structures via hydrogen bonding which in turn stabilizes the structure and promote multimerization (Hoffner, et al. 2007).

Also, the transglutaminase model attempts to provide a mechanism for aggregate formation in Huntington's disease. Transglutaminases are enzymes that cross-link glutamine residues (Kahlem, et al. 1998). Early studies implicated Htt as a transglutaminase-substrate and showed that cross-linking via transglutaminase increased with increasing length of the polyglutamine expansion (Kahlem, et al. 1998). Also, in vivo studies have shown an increase in transglutaminase activity in the brains of HD patients (Gil and Rego. 2008, Karpuj, et al. 2002). Thus, the HD expanded polyglutamine tract may cause the cross linking of mHtt and polyglutamine containing proteins in a transglutaminase-mediated manner. While evidence of the Polar Zipper and Transglutaminase models are well documented it is likely that their contribution to aggregate formation is not mutually exclusive. Despite mHtt expression throughout the body, the regional specificity of neuronal toxicity in the striatum and cortex, does create

an interesting paradox suggesting that polyQ expansion and protein aggregation are involved in cellular toxicity.

The interaction of several key intracellular proteins with mHtt and their sequestration into neuronal aggregates has been shown to disrupt several cellular processes and contribute to the downstream neuronal toxicity seen in HD. Cummings et al. (2001) showed a mHtt induced upregulation of molecular chaperones known as the heat shock proteins (HSPs) which function to refold misfolded proteins. The upregulation of HSPs may represent a cellular attempt to alleviate the polyQ induced aggregation. However a subsequent study revealed the sequestration of HSPs 40 and 70 into the cytosolic aggregates which over time would result in an eventual loss of overall chaperone function (Schaffar, et al. 2004). Also, the sequestration of key regulatory and catalytic elements of the proteasome into cytosolic aggregates has been shown to occur in HD (Wytttenbach, et al. 2002). A study by Bennett et al. (2007), revealed the co-localization of polyubiquitinated proteins within cytosolic neuronal aggregates during the early pathological stages of HD. These findings suggest that an aggregate induced dysfunction of the ubiquitin-proteasome system occurs in HD.

1.3.2 Transcriptional deregulation

Transcriptional deregulation has also been associated with HD and is believed to contribute to downstream pathology. mHtt has been shown to bind abnormally to several nuclear proteins and transcription factors such as TATA binding protein (TBP) and CREB [cyclic-adenosine monophosphate response element binding protein] binding protein (CBP) (Schaffar, et al. 2004). Protease cleavage sites for caspases and calpain

have been identified within the Huntingtin protein (Kim, et al. 2001). With mHtt expression, proteolysis has been shown to increase proportionally with increasing polyQ expansion, producing N-terminal toxic fragments that are more prone to aggregation and passively diffuse into the nucleus where they can negatively regulate nuclear proteins and transcription factors (Ratovitski, et al. 2009). Particularly the deregulation of several key transcription factors involved in mitochondrial function has been a well documented phenomena believed to contribute to mitochondrial perturbation and downstream HD neuronal toxicity (Quintanilla and Johnson. 2009).

1.3.3 Aberrant mitochondrial function

Specifically, peroxisome proliferator-activated receptor- λ coactivator (PGC-1 α) is a transcriptional co-activator that regulates the expression of proteins involved in mitochondrial respiration (St-Pierre, et al. 2006). Several studies have shown a mHtt specific decrease in PGC-1 α . Also, the N-terminal truncated form of mHtt has been shown to bind to and alter the function of nuclear transcription protein known CBP (Riley and Orr. 2006). By binding to CBP, mHtt decreases expression of mitochondrial genes including those associated with complex I and III of the electron transport chain (ETC) (Sugars, et al. 2004). Aside from transcriptional deregulation there have also been well-documented functional abnormalities associated with the mitochondria and mHtt expression. In human HD brains a significant decrease in the activity of complex II and IV of the ETC have been observed as compared to non-diseased control brains (Gu et al. 1996). Also, an inverse relationship between CAG length and mitochondrial produced ATP has been documented in human cell lines, where the longer the length of polyglutamine expansion the less ATP produced (Seong, et al. 2005). Thus, perturbed

mitochondrial function has been implicated as a major contributor to downstream events resulting in HD pathology.

1.3.4 Oxidative stress

One major result of aberrant mitochondrial function is oxidative stress which is well documented in HD. Oxidative stress occurs when the rate at which reactive oxygen species (ROS) are produced exceeds the rate at which they are detoxified (Cumming, et al. 2004). ROS are a natural byproduct of intracellular processes such as metabolism and the CNS is particularly susceptible to oxidative damage because of its high rate of oxygen utilization (Ding and Keller. 2001). Oxidative stress can lead to irreversible damage of DNA, proteins and lipids. There is a significant body of literature linking oxidative stress with HD (Trushina and McMurray. 2007, Ding and Keller. 2001, Sayre et al. 2008). Studies of post-mortem brain tissue from HD patients and transgenic HD mice (R6/2) revealed elevated levels of oxidative damage products such as malondialdehyde, 8-hydroxydeoxyguanosine and 3-nitrotyrosine in areas of degeneration (Sultana and Butterfield. 2008, Bogdanov, et al. 2001). Aside from generating vital ATP for cellular metabolic processes, mitochondria are also regulators of cell death and are a major site of ROS production (Sorolla, et al. 2008). The deficiencies in mitochondrial complexes, either from transcriptional deregulation or functional abnormalities, have been shown to elevate ROS levels and increase protein oxidation which promotes cell death (Sorolla, et al. 2008). Also, a mHtt/mitochondria interaction has also been identified that alters mitochondrial calcium buffering, resulting in mitochondria dysfunction and an increase in ROS. Both the increase in oxidative stress markers in the striatum and cortex as well as immunocytochemical evidence for oxidative damage to

biological molecules implicate oxidative stress in HD (Sayre, et al. 2008). Transcriptional up-regulation of antioxidant protein mRNA, such as peroxiredoxins 1, 2 and 6 as well as glutathione peroxidase occurs in the brain of HD patients, providing further evidence that a protective response is elicited by the presence of elevated ROS (Sorolla, et al. 2008). Interestingly, even though there is an upregulation of antioxidants in HD, post-mortem analysis of human brain tissue has shown that elevated oxidative damage to proteins in the striatum and cortex still occurs (Schilling, et al. 2001). Thus, the protective anti-oxidant response triggered by elevated ROS in the brains of HD patients may not be sufficient to deal with the oxidative stress situation, or perhaps the antioxidant proteins undergo post-translational oxidative modifications rendering them inactive and unable to detoxify ROS.

1.4 Proposed mechanism for HD neuronal toxicity

A known post-translational oxidative modification is disulfide bond formation (DSBF). ROS have been shown to cause several oxidative modifications to amino acid side chains of proteins including carbonylation, nitrosylation and oxidation of methionine to methionine sulfoxide (Cumming, et al. 2004). Also, certain proteins containing cysteine sulfhydryl groups (Cys-SH) can be reversibly oxidized to sulfenic acids and disulfide bonds (DSB), or over oxidized irreversibly to sulfinic and sulfonic acids; all of which can result in an altered structure and/or function of the oxidized proteins (Cumming, et al. 2004). While DSBF was primarily thought to occur in proteins contained in the oxidizing environment of the endoplasmic reticulum, DSBF is now well documented to occur in cytoplasmic proteins and play a crucial role in cell signaling and antioxidant defense (Cumming, et al. 2004). Specifically the tumor necrosis- α -induced

signaling pathway has been shown to have downstream kinase activity regulated by H_2O_2 , a common ROS within the cell (Liu, et al. 2000). Also, in addition to cell signaling many redox sensitive proteins such as the glutathione (GSH)/ glutaredoxin (GRx) antioxidant system makes use of transient DSBF while catalyzing the reduction of thiol groups (Kalinina, et al. 2008). In addition, increased DSBF and over oxidation of proteins has been shown to promote misfolding and aggregate formation that is resistant to proteolysis (Ding and Keller. 2001). Thus, DSBF in response to oxidative stress may be a mechanism that promotes aberrant protein function and aggregate-induced toxicity that may have relevance to the progression of HD. However, no evidence to date has been presented showing that alterations in protein DSBF occurs in an HD context.

1.5 Current HD treatments

While there is currently no cure or effective treatment for HD, the vast amount of literature implicating oxidative stress as a key player in disease progression has made the study of antioxidant therapy a main focus of treatment biology surrounding HD. The mitochondrial enzyme known as Coenzyme Q10 (CoQ10) has been implicated as a neuroprotectant in several preclinical transgenic mouse studies (Schilling, et al. 2001). CoQ10 is an enzyme found within the inner mitochondrial membrane and is the first enzyme electrons must interact with to progress along the ETC, thus CoQ10 plays a vital role in ETC efficiency and energy production (Young, et al. 2007). Transgenic mouse models of HD revealed that CoQ10 supplementation significantly decreased neuronal damage and loss (Young, et al. 2007). However, administration of CoQ10 to HD patients in clinical trials revealed no significant change in patient symptoms or prevention of neurodegeneration (Young, et al. 2007).

While it is not known mechanistically whether mitochondrial dysfunction contributes to a downstream increase in ROS or initially, an increase in ROS causes the mitochondrial dysfunction, antioxidants have strongly been considered as a potential therapeutic strategy to treat HD. Several thiol-antioxidants such as cystamine and N-acetyl cysteine (NAC) which remove ROS or inhibit oxidation of proteins have been shown to attenuate the HD phenotype in cell culture models (Fontaine, et al. 2000, Fox, et al. 2004, Mao, et al. 2006). However, mechanistically how these antioxidants exert their neuroprotection remains poorly understood.

1.6 Hypothesis and investigative plan

It is hypothesized that changes in disulfide bond formation (either induction or diminishment) will occur in response to oxidative stress induced by mHtt expression. Also, thiol based antioxidants will inhibit this HD induced aberrant disulfide bond formation and cellular toxicity.

Several HD models exist in flies, mice and cell culture. The clonal rat pheochromocytoma cell line (PC12) is a useful model of HD because it is well-characterized in the literature and exhibits many characteristics of mature neurons (Aiken, et al. 2004). Using PC12 cells, this study plans to (1) establish a change in oxidative status specific to mHtt^{103Q} expression using a mitochondrial specific ROS detection dye (MitoTracker Red) (2) determine oxidative stress induced changes in the PC12 disulfide proteome using two-dimensional (2D) redox polyacrylamide gel electrophoresis (PAGE), (3) identify DSBP that are altered by mHtt^{103Q} expression using mass spectrometry, (4) confirm changes in DSBF specific to mHtt^{103Q} expression using

1D immunoblot analysis under nonreducing and reducing conditions and (5) using the thiol-based compounds cystamine, beta-mercaptoethanol (BME), dithiothreitol (DTT) and penicillamine, analyze compound specific changes in PC12 cell viability with the colorimetric 3-(4,5-Dimethylthiazol-2-yl)-2,5-diphenyltetrazolium bromide (MTT assay), confirmed with a trypan blue assay. Lastly, the effects of the thiol-based compounds on the disulfide proteome using 2D Redox PAGE will be analyzed and confirmed by 1D immunoblot analysis.

Chapter 2

Materials and Methods

2.1 Cell culture and transgene induction.

A PC12 nerve-like cell line was obtained from Dr. Leslie Thompson (University of California at Irvine) that is stably transfected with a plasmid encoding the entire exon 1 of the HD gene with either a 25 (non-pathogenic) or 103 (pathogenic) polyQ repeat fused in frame to the coding sequence for the enhanced GFP at the carboxy terminus. Transcription of the transgene is driven by an ecdysone regulated promoter that can be turned on by the addition of ecdysone or tebufenicide (an ecdysone analogue). PC12 cells were grown in Dulbecco's modified eagles medium (DMEM) containing 10% horse serum, 5% fetal bovine serum and 1% penicillin/streptomycin and incubated in a 37.5° C humidified CO₂ incubator with 5% CO₂/ 95% air. Cells were maintained at no greater than 50% confluence. Induction of the 25Q (Htt^{25Q}) or 103Q (mHtt^{103Q}) transgenes in all experiments was accomplished through the addition of 2.5 μM tebufenocide [in a dimethylsulfoxide (DMSO) vehicle] with various induction times of 1, 2, 3 days depending on the experiment, as specified in the corresponding section. DMSO alone was also added as a control at the same time of transgene induction for 2D Redox PAGE and 1D immunoblot analysis. A trypan blue assay was initially used to test neuronal toxicity for Htt^{25Q} and mHtt^{103Q} cell lines after 2.5 μM tebufenocide induction to confirm the absence of cell death in the non-pathogenic cell line (Htt^{25Q}) and approximately 20,

50 and 80% cell death in the pathogenic cell line (mHtt^{103Q}) after 1, 2 and 3 days respectively.

2.2 Determination of mitochondrial produced ROS

To visualize mitochondrial produced ROS, cells were seeded at 4×10^5 in 6-well dishes and induced with 2.5 μ M tebufenocid. After 2 days, media was aspirated and cells were incubated in media containing 100 nM MitoTracker Red CM-H₂XROS (Molecular Probes) for 20 minutes (min) at 37.5° C in a humidified CO₂ incubator with 5% CO₂/ 95% air. The MitoTracker Red was then removed, cells were washed with PBS and phenol red free media was added to the culture prior to visualization with fluorescent microscopy (Zeiss).

2.3 Cell fractionation and protein lysate preparation.

For 2D Redox PAGE and 1D immunoblot experiments, all cells were seeded at 2.0×10^6 cells in 10 cm dishes and transgene expression was induced 24 hours (h) after seeding. Cells were harvested in Triton-X100 buffer at the 2 day time point (2D redox PAGE) or the 1, 2 and 3 day time points (1D immunoblot). Cells were washed with cold phosphate buffered saline (PBS), incubated for 3 min with PBS containing 40 mM iodoacetamide (IA) and scraped in the presence of 100 μ L of Triton-X100 extraction buffer [50 mM Tris pH 7.5, 1% Triton-X100, 1mM phenylmethanesulfonylfluoride (PMSF), 40 mM iodoacetamide]. The cell suspension was rocked on ice for 20 min and centrifuged at 15 000 X G for 10 min. Subsequently the supernatant (containing all soluble proteins) was aliquoted and frozen at -80° C.

2.4 Cell lysate protein content.

Protein content of the soluble fraction of the cell lysates was determined using the colorimetric BioRad DC Protein Assay Kit.

2.5 Two-dimensional Redox PAGE.

Protein lysates (300 μ g) for Htt^{25Q} and mHtt^{103Q}, uninduced and induced conditions were initially resolved for 5 h at constant current, under non-reducing conditions through a 1.5 mm, 12% polyacrylamide gel using a Hoefer SE600 electrophoresis apparatus (San Francisco). Following electrophoresis in the first dimension, gel strips containing resolved proteins were excised and immersed in sodium-dodecyl sulphate (SDS) sample buffer (0.5 M Tris-HCL, 5% glycerol and 2% SDS) containing 100 mM dithiothreitol (DTT) for 20 min at room temperature. Gel strips were then washed with SDS-running buffer and immersed for 10 min in SDS sample buffer containing 100 mM IA. Each gel strip was then applied horizontally to a second gel (1.5 mm, 12% polyacrylamide) and run for 14 h at constant current (10 mA/gel). After electrophoresis in the second dimension, gels were fixed in 50% methanol overnight before silver-staining.*

2.5.1 Two-dimensional Redox PAGE: positive and negative controls

Cell lysates were obtained for both positive and negative controls as outlined in section 2.3. Cells plated for the positive control samples were not induced and were exposed 1 day after seeding to 10 mM hydrogen peroxide (H₂O₂). Positive control samples were

* Explanation of 2D redox-PAGE map can be found in Appendix 1, Supplemenatry Figure 2.

subject to 2D Redox PAGE as outlined in section 2.5. Negative control samples were analyzed by 2D Redox PAGE under reducing conditions in both the first and the second dimension with 100 mM DTT.

2.6 DSB visualization.

DSBPs separated by Redox 2D-PAGE were visualized by silver staining. Gels that had previously been fixed overnight with 50% methanol were washed (3 x 20 min) in water and sensitized for 1 min with 0.02% sodium thiosulfate (Sigma). Sensitized gels were then washed (3 x 1min) and incubated with 0.1% silver nitrate solution (Sigma) for 30 min. After impregnation of the silver, gels were washed (3 x 1 min) and developed in 35% formaldehyde and 2% sodium carbonate. Gels were developed for approximately 8 min, or until desired intensity of staining was achieved and development was stopped using 5% acetic acid.

2.7 Identification of redox-sensitive proteins.

Gel spots from redox 2D gels were excised and in-gel digested with trypsin. In-gel digestion was performed using a MassPREP automated digester station (PerkinElmer). Gel pieces silver de-stained using a 50 mM sodium thiosulphate 5 hydrate and 15 mM potassium ferricyanide solution, which was followed by protein reduction using 10 mM dithiotreitol (DTT), alkylation using 55 mM iodoacetamide (IA), and tryptic digestion. Peptides were extracted using a solution of 1% formic acid and 2% acetonitrile and lyophilized. Prior to mass spectrometry analysis, dried peptide samples were re-dissolved in a 10% acetonitrile and 0.1 % TFA (trifluoroacetic acid).

Aliquots of digested samples were mixed with an equal volume of MALDI matrix (α -cyano-4-hydroxycinnamic acid (CHCA), was prepared as 5 mg/mL in 6mM ammonium phosphate monobasic, 50% acetonitrile, 0.1 % trifluoroacetic acid) at a 1:1 ratio (v/v). Mass Spectrometry data were obtained using a 4700 Proteomics Analyzer, MALDI *TOF* (Applied Biosystems, Foster City, CA, USA). Data acquisition and data processing were respectively done using 4000 Series Explorer and Data Explorer (both from Applied Biosystems). The instrument is equipped with a 355 nm Nd:YAG laser; the laser rate is 200 Hz. Reflectron positive ion mode was used and the instrument was calibrated at 25 ppm mass tolerance and monoisotopic masses were determined with NCBI rat protein database using the Mascot program. Each mass spectrum was collected as a sum of 1000 shots.

2.8 Immunoblot analysis.

Triton-X soluble protein extracts (30 ug) were resolved by 12% nonreducing and reducing PAGE using the OmniPage-Mini Wide electrophoresis apparatus (Clever Scientific). Soluble protein lysates resolved under reducing conditions were treated with 100 mM DTT and 2% Beta-mercaptoethanol (BME) and boiled for 5 min. Gels were electroblotted onto Immobilon-P membrane (Millipore, Bedford, MA), blocked with 1% milk and 3% bovine serum albumin (BSA, Sigma) in tris-buffered saline (TBST). Membranes were incubated with polyclonal rabbit antibodies against Prx-1 (Ab Frontier, South Korea), GFP (Sigma, St. Louis, USA) and actin (Cell Signaling) overnight. Following incubation, membranes were washed (3 x 5 min) with Tris-buffered saline and further hybridized with horse-radish peroxidase-conjugated secondary antibodies

(BioRad). Detection was performed using Pierce ECL Western blotting detection reagents (ThermoScientific) and a ChemiDoc digital imaging system (BioRad).

2.9 MTT and trypan blue cell viability assays

For MTT assays cells were seeded in quadruplicate at 10 000 cells/well in 96-well plates. The thiol-based compounds Cystamine, BME, DMP, and Penacillamine (Sigma) were added at various concentrations (0.0001, 0.001, 0.005, 0.01, 0.05, 0.1, 0.5, 1, 1 mM) to 96-well plates 24 h after cells were seeded. One hour after compound exposure, transgene expression was induced with 2.5 μ M tebufenocide.

The viability of cells at the 2 day time-point was determined with the addition of 10 μ L of a 5g/ml MTT (Sigma) stock in PBS and incubation at 37°C for four hours. The purple formazan product of MTT was release from cells by the addition of 100 μ L of solubilization buffer (20% SDS, 50% dimethylformamide). Absorbance was measured at a test wavelength of 595 nm and reference wavelength of 655 nm using a microplate reader (BioRad).

Cellular viability under the same conditions was confirmed using Trypan Blue Assay with cells seeded at 1.0×10^5 in 6-well dishes. Following trypsinization, equal volumes of cell suspension and 0.4% trypan blue (Sigma) were incubated at room temperature for 5 min and cells excluding dye were counted using a hemocytometer to measure cell viability

2.10 Analysis of DMP specific changes in the PC12 disulfide proteome.

Attenuation of mHtt^{103Q} induced changes in the disulfide proteome were analyzed in the presence of 0.1 mM DMP. Cells were seeded according to same methodology

above, incubated with 0.1 mM DMP 1 h prior to induction with 2.5 μ M tebufenocide and harvested after 2 days. DMP treated cell lysates were then analyzed by 2D Redox PAGE and Prx-1 specific 1D immunoblot analysis (as described above) and compared to the original 2D profile (without DMP) or 1D immunoblots (without DMP) to indicate DMP specific changes.

Chapter 3

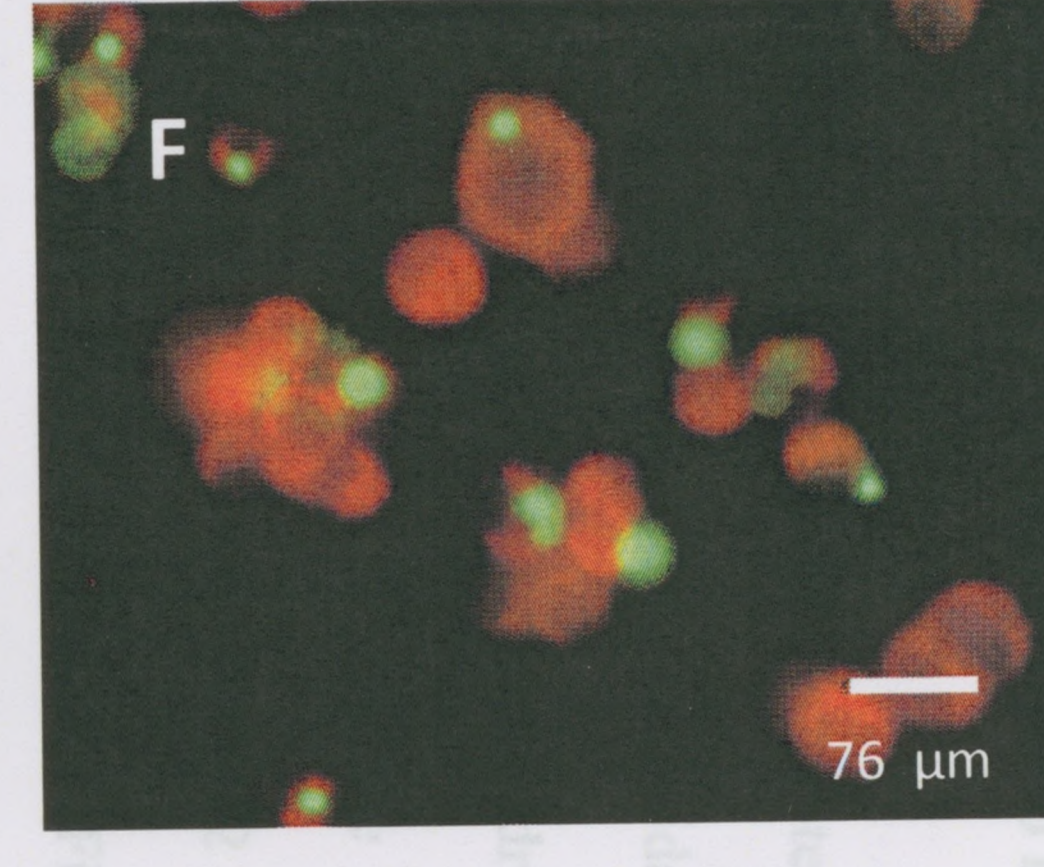
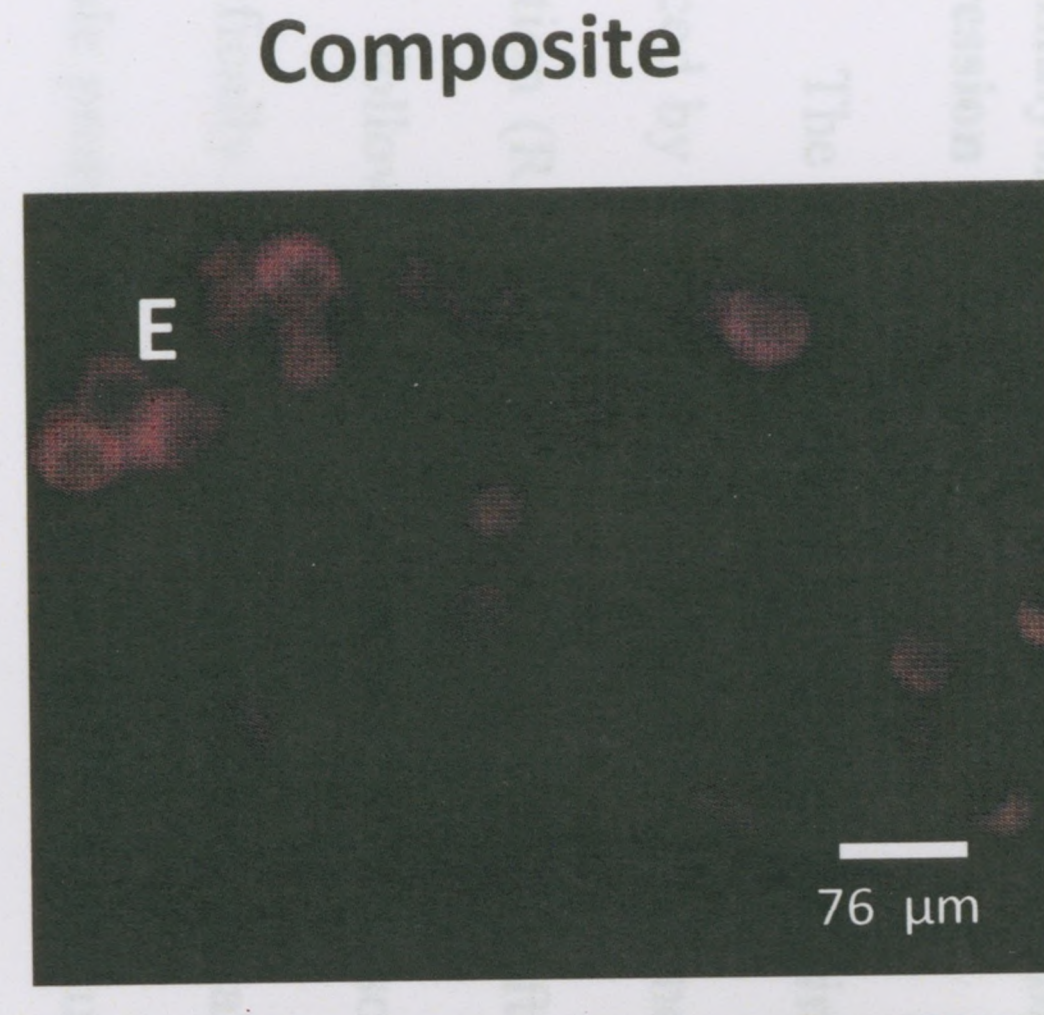
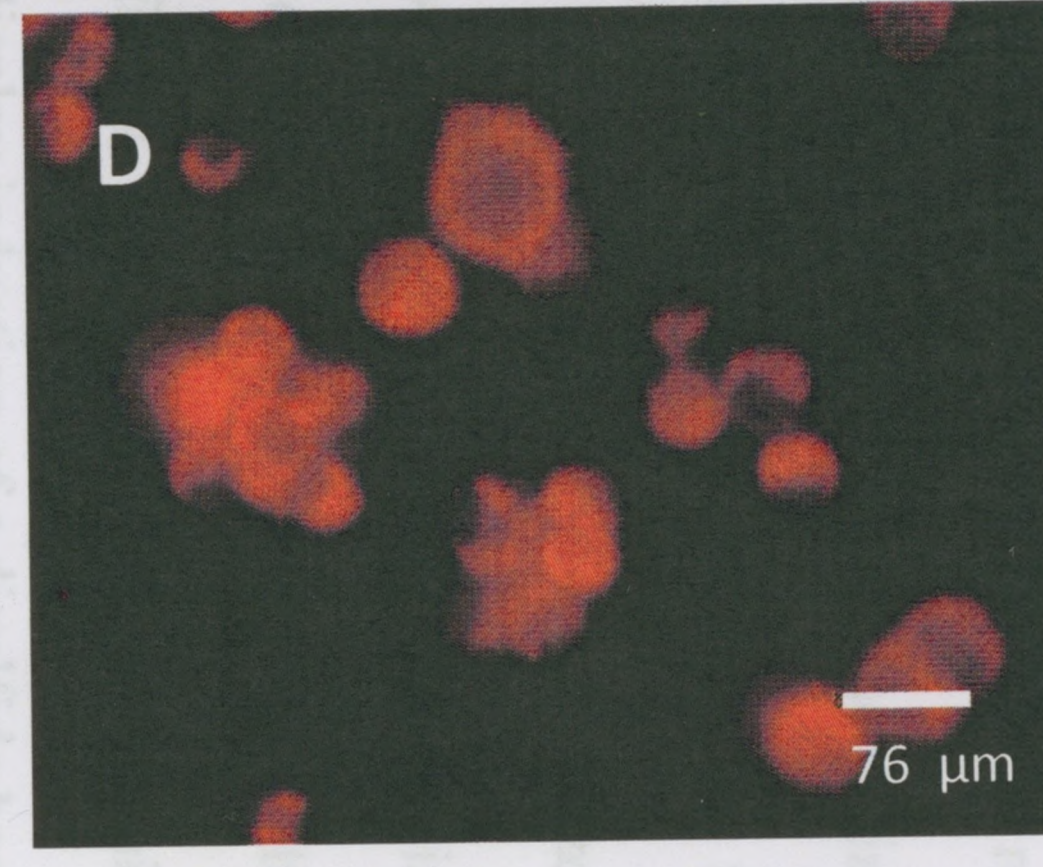
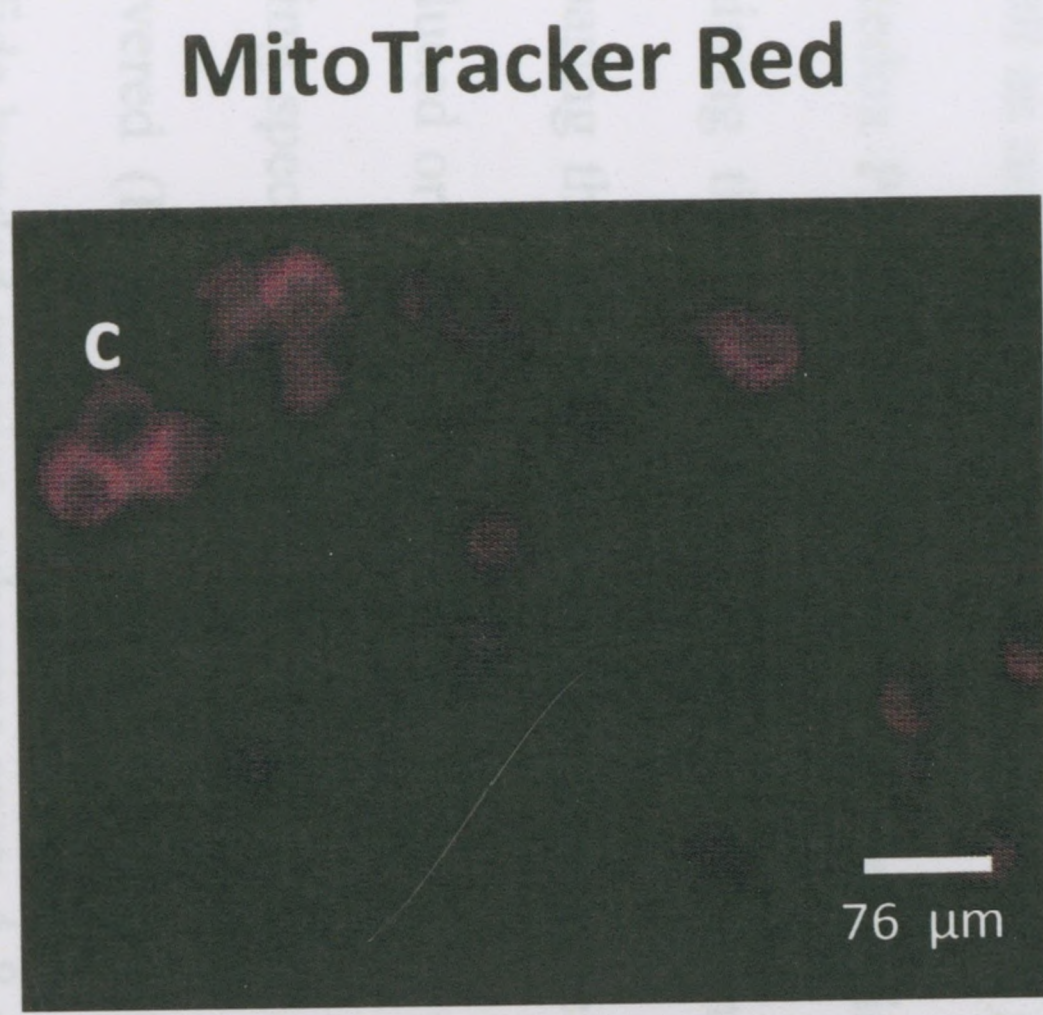
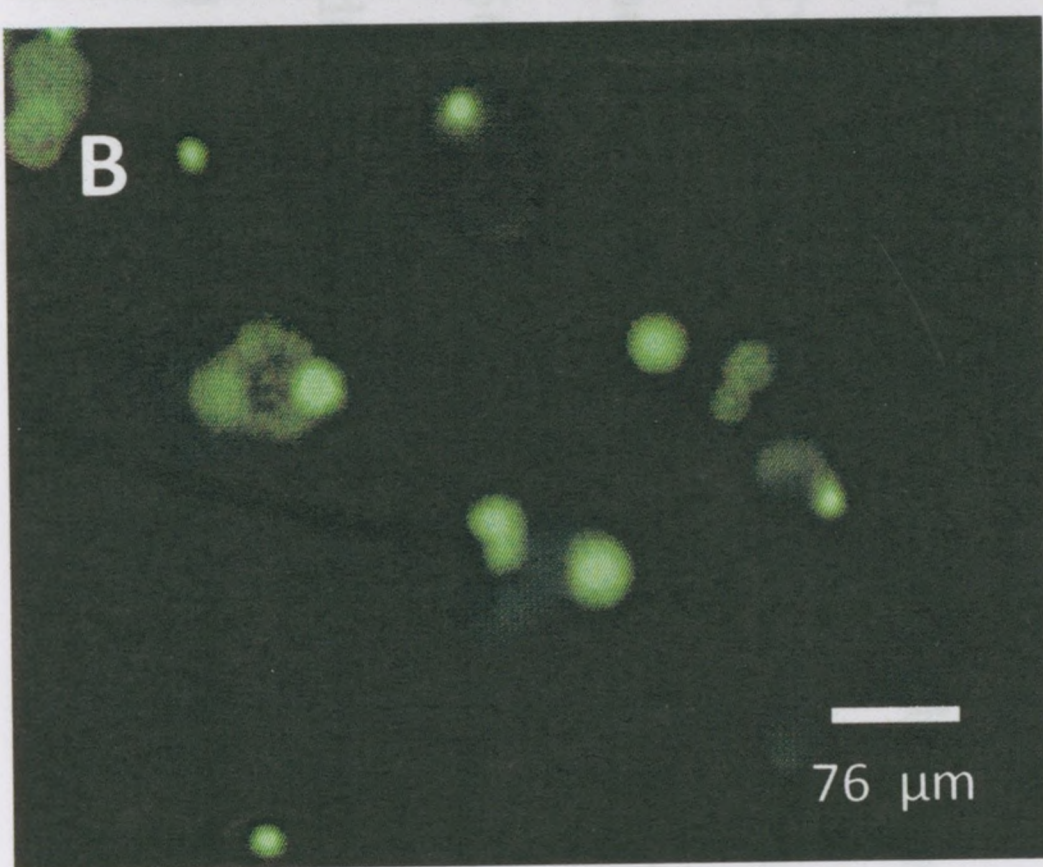
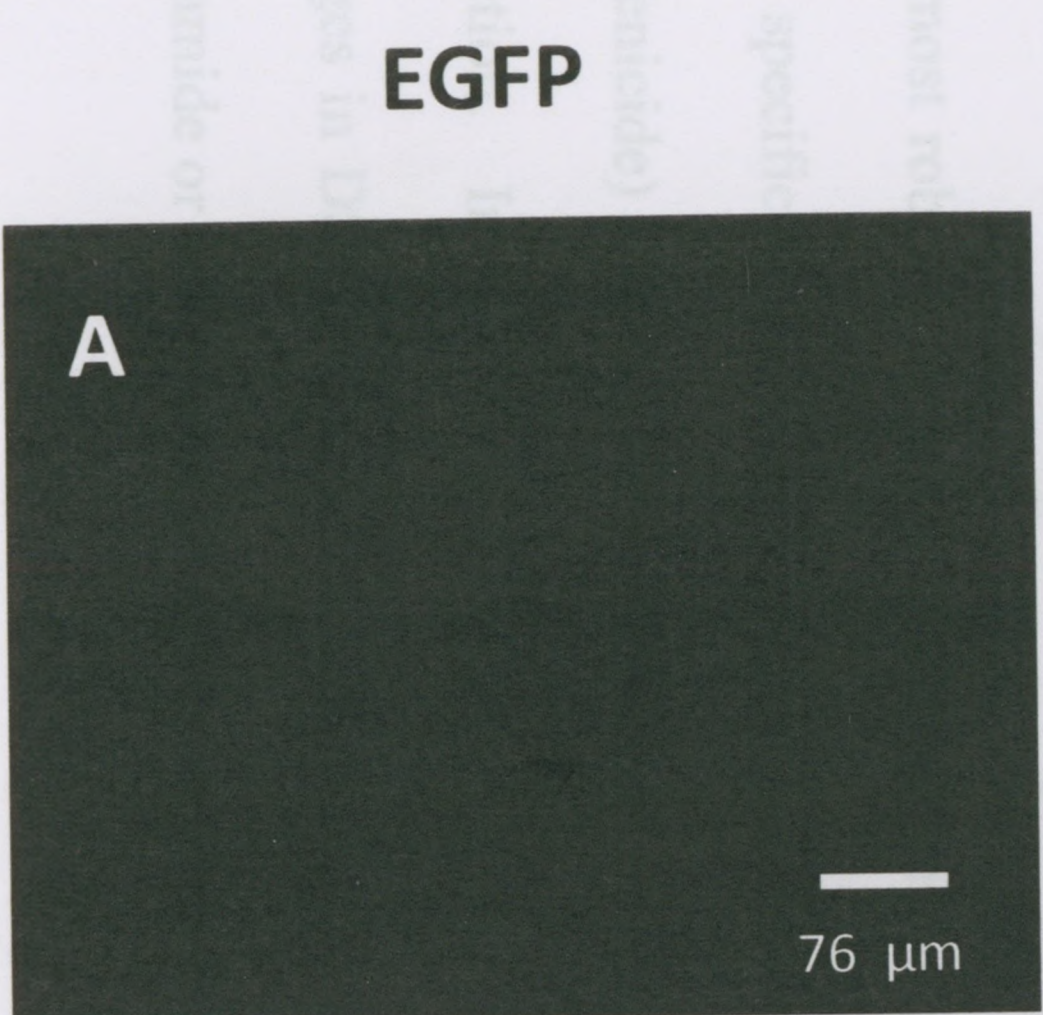
Results

3.1 mHtt^{103Q} and Mitochondrial Produced ROS in PC12 cells.

While oxidative stress is a well documented hallmark of HD pathology across a host of cell models, perturbed mitochondrial function leading to an increase in ROS production has never before been shown using MitoTracker Red CM-H₂XRos in the PC12 cell model. Upon incubation, the reduced probe MitoTracker Red CM-H₂XRos passively diffuses across the cell membrane and is taken up into actively respiring mitochondria, oxidizing the probe and causing it to fluoresce. After a 2 day induction with 2.5 μ M tebufenocid, PC12 cells showed a dramatic increase in mitochondrial produced ROS specific to mHtt^{103Q} (Figure 1. D) as compared to the uninduced control that was also incubated with MitoTracker Red CM-H₂XRos (Figure 1. C). mHtt^{103Q} expression was confirmed with EGFP fluorescence under induced conditions (Figure 1. B) as compared to its absence under uninduced conditions (Figure 1. A). Also, the increase in mitochondrial produced ROS appears to be roughly correlated with mHtt^{103Q} aggregate formation as visualized with the overlaid images (Figure 1. F).

Figure 1.

Effect of PC12 mHtt^{103Q} induction on mitochondrial produced reactive oxygen species. Control, uninduced (-) PC12 cells (A) showing no expression of the mHtt^{103Q} transgene as compared to induced (+) PC12 cells (B) with robust transgene expression and formation of intracellular aggregates, visualized with EGFP fluorescence. Control uninduced cells show relatively little mitochondrial ROS production (C) as compared to cells expressing mHtt^{103Q} (D). Aggregate formation and intensity of mitochondrial ROS production appears to be roughly correlated by comparing control (E) and induced (F) overlays.



-

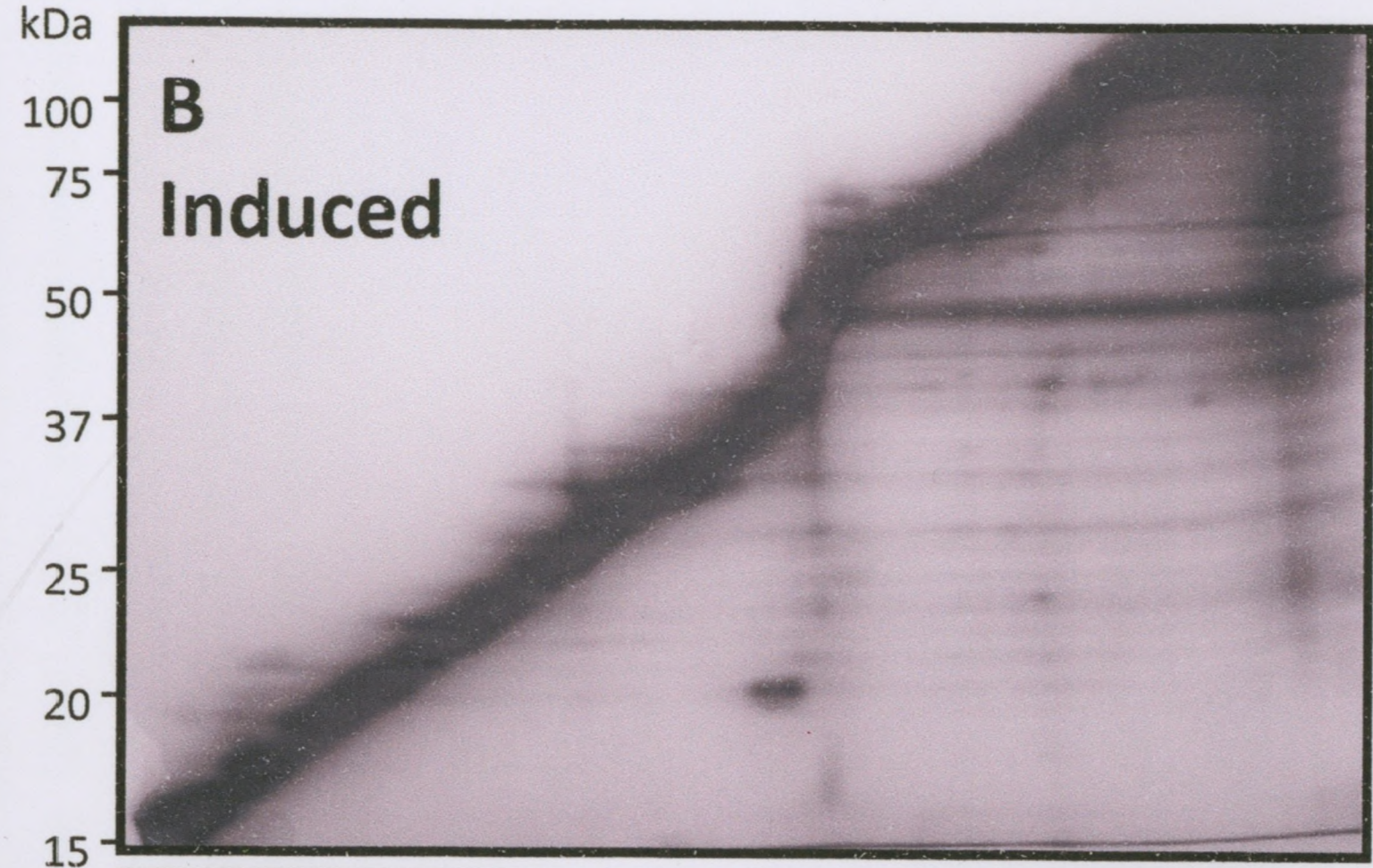
+

3.2 Analysis of changes in the PC12 soluble disulfide proteome specific to mHtt expression

The modification or loss of cysteine sulfhydryl groups within proteins can be induced by a wide range of ROS and is one of the first responses to an oxidative stress situation (R.C Cumming, et al. 2004). After observing elevated mitochondrial derived ROS following mHtt expression, we sought to determine if cysteine oxidation, specifically disulfide bond formation, is altered in mHtt expressing PC12 cells. The soluble protein fractions from Htt^{25Q} uninduced (Figure 2. A) and induced (Figure 2. B) as well as mHtt^{103Q} uninduced (Figure 2. C) and induced (Figure 2. D) were resolved by 2D Redox PAGE. The resulting silver-stained gels revealed a prominent diagonal line containing the majority of soluble proteins that do not contain disulfide bonds. By comparing the appearance or disappearance of proteins in the off-diagonal zones under uninduced or induced conditions (Figure 2) we were able to discern changes in disulfide bonding specific to mHtt^{103Q}. Eight robust changes in DSBF specific to mHtt^{103Q} were discovered (Figure 2. D, spots 1-8). Specifically, spots 1-3 reveal a diminishment in disulfide bonded species, whereas spots 4-8 display induction of a disulfide bonded form. The most robust change is notably the diminishment of spot 1. The changes in DSBF were specific to mHtt^{103Q} expression as DMSO alone (the vehicle used to dissolve tebufenicide) was added to the control uninduced cells at the same time of transgene induction. In addition, induction of Htt^{25Q} expression promoted relatively modest changes in DSBF relative to mHtt^{103Q} induced changes. In order to ensure that the acrylamide or 2D Redox PAGE technique did not artificially induce disulfide bonding,

Figure 2.

Separation of disulfide bonded proteins from the soluble Triton-X100 fraction by 2D Redox PAGE. PC12 soluble protein extracts were resolved in the first dimension under nonreducing conditions, in the second dimension under reducing conditions and visualized with silver staining. Soluble proteins resolved represent Htt^{25Q} non-induced (A), Htt^{25Q} induced (B), mHtt^{103Q} non-induced (C) and mHtt^{103Q} induced (D). Transcription of the transgene to produce Htt^{25Q} (B) or mHtt^{103Q} (D) was induced by the addition of 2.5 μ M of tebufenocid 2 days prior to harvesting. Non-induced control groups were treated with DMSO a tebufenocid vehicle (A and C). Changes in DSB specific to mHtt have been numbered 1-8 (N=3).



Reducing

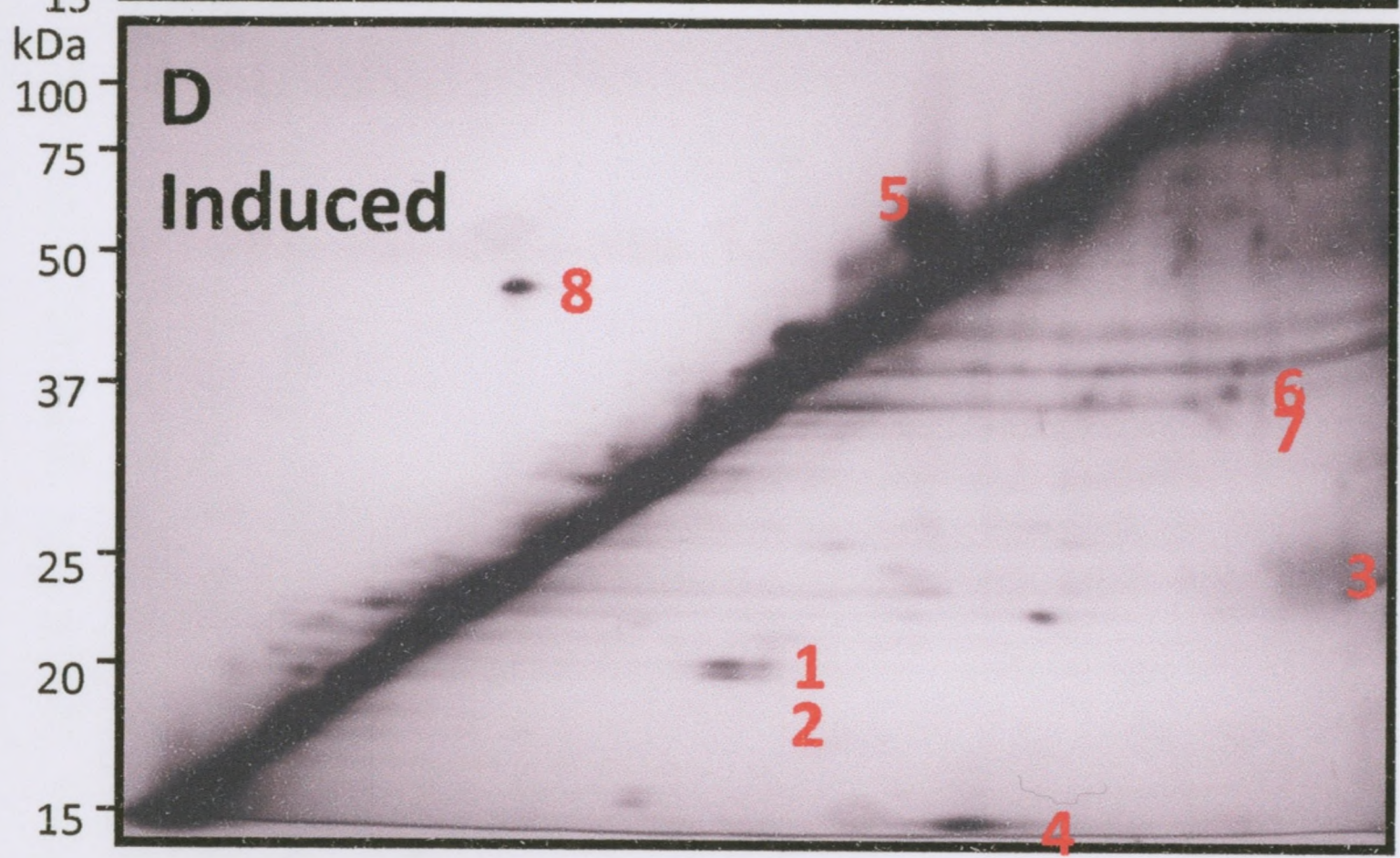
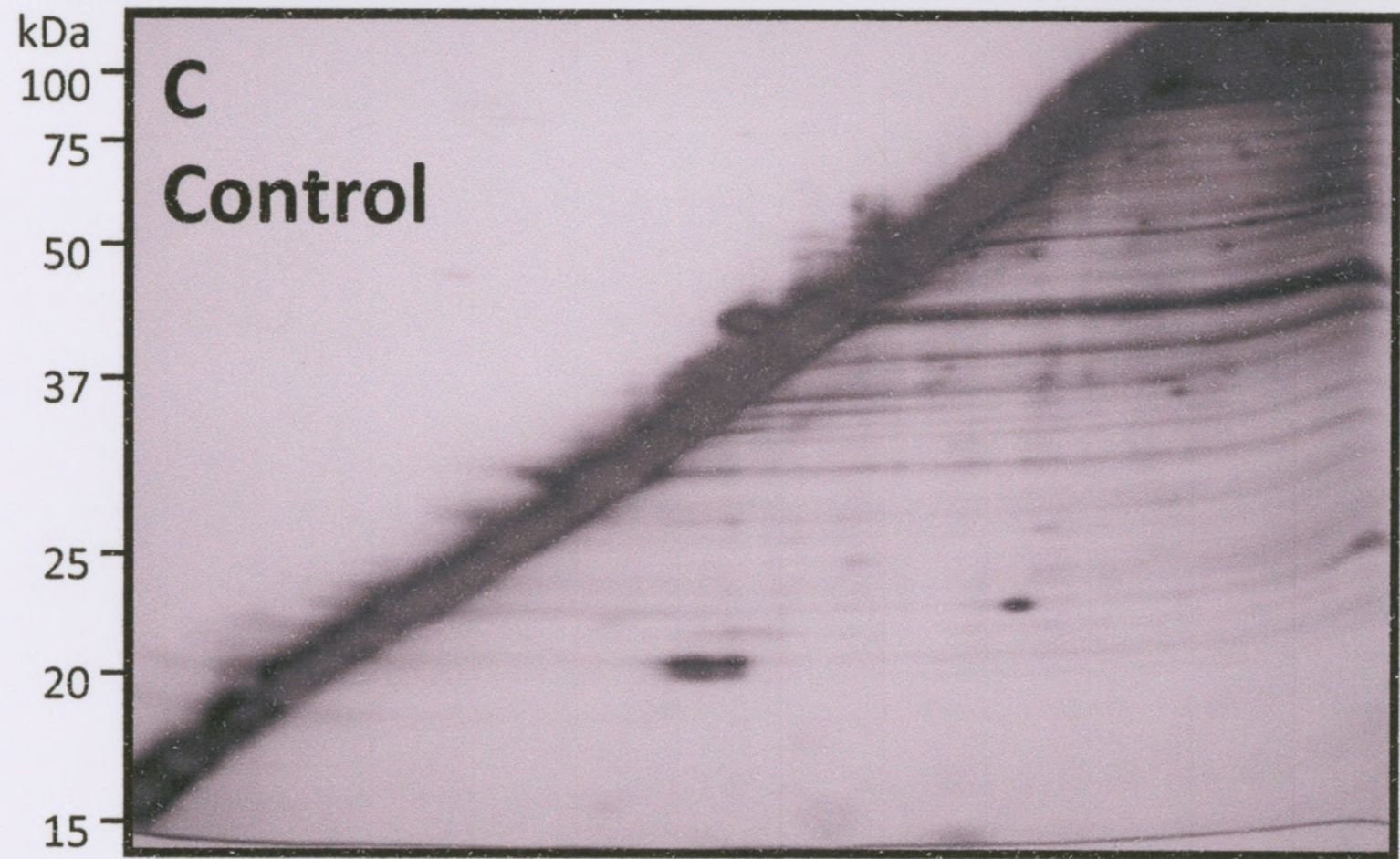


Figure 3.

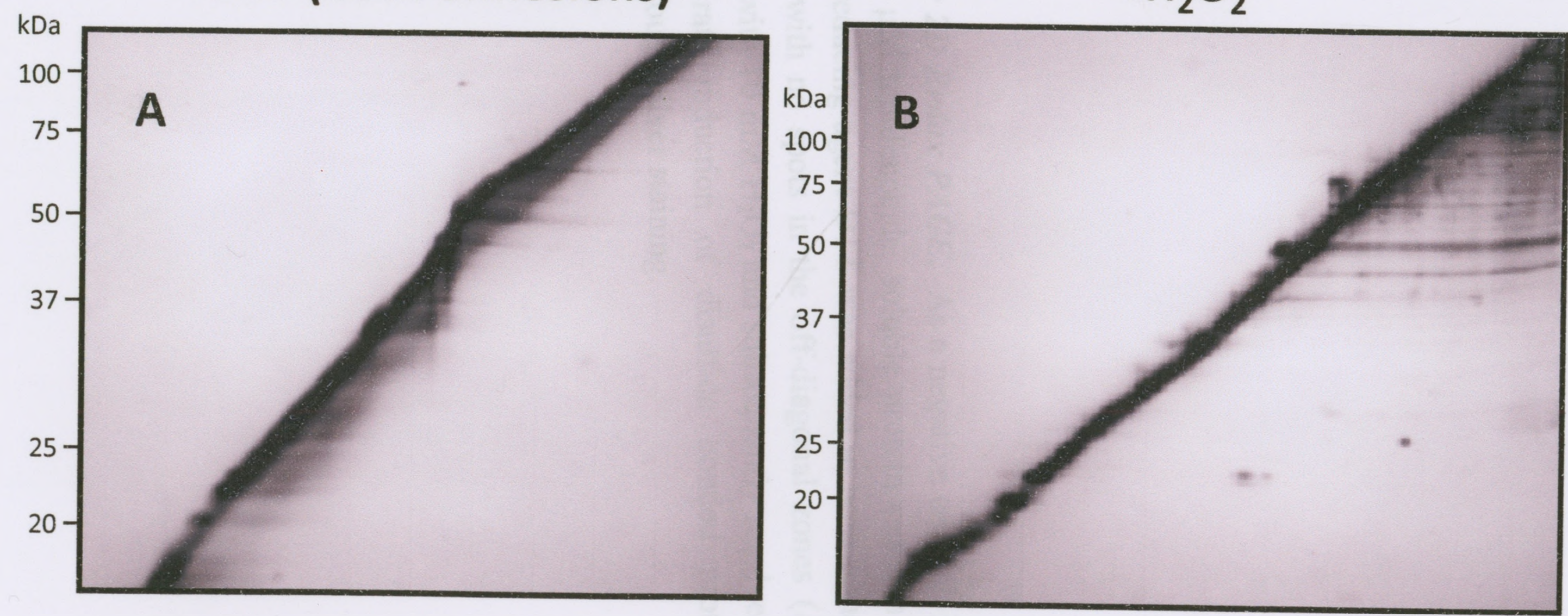
Negative and positive controls for 2D Redox PAGE. As a negative control, PC12 cells were induced for 2 days with 2.5 μM tebufenocid, soluble protein extracts were run using 2D redox PAGE where the reducing agent DTT was added in both dimensions to reveal a prominent diagonal line with no spots in the off-diagonal zones (A). As a positive control cells were treated with 10 mM H_2O_2 and subsequently resolved with 2D Redox PAGE showing a moderate induction of disulfide bonded proteins (B). Visualization was accomplished through silver staining.

Figure 3.

Negative and positive controls for 2D redox PAGE were induced for 2 days with 2.5 μM H₂O₂. The results revealed a prominent diagonal line with positive control cells were treated with Redox PAGE showing a prominent diagonal line with visualization was accomplished.

+DTT (both dimesions)

+H₂O₂



+H₂O₂

+DTT (both dimesions)

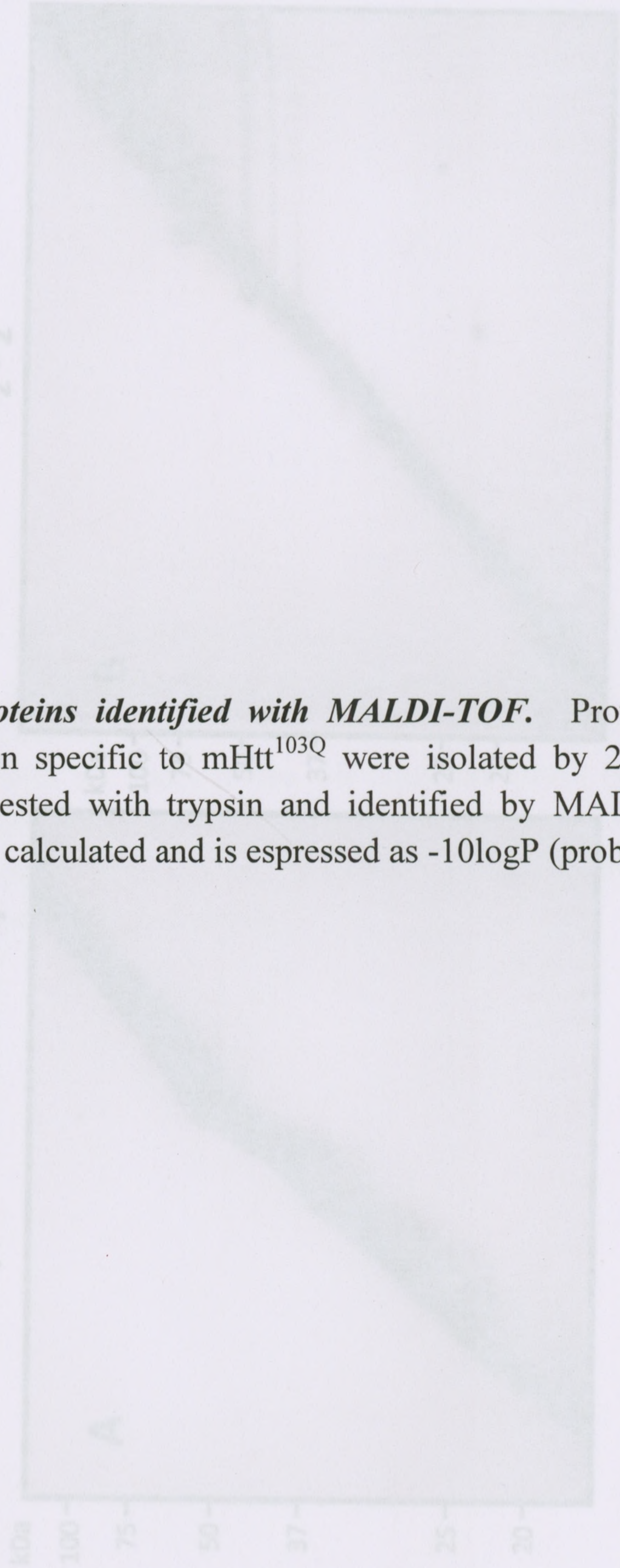


Table 1.

Summary of disulfide bonded proteins identified with MALDI-TOF. Proteins that underwent disulfide bond formation specific to mHtt^{103Q} were isolated by 2D Redox PAGE, silver-destained, in-gel digested with trypsin and identified by MALDI-TOF. MOWSE probability score was also calculated and is expressed as -10logP (probability).

soluble protein lysates were treated in both dimensions with the reducing agent DTT. As expected, a clear diagonal line was revealed with no spots in the off-diagonal zones (Figure 3, A). Also, at a positive control, extracts from cells were exposed to H₂O₂ revealed a rate increase in disulfide bonded species following Redox 2D-PAGE analysis.

Table 1.

Protein	Spot No.	MOWSE Score	Function	+/-
Peroxiredoxin 1	1	183	Antioxidant	-
Peroxiredoxin 2	2	54	Antioxidant	-
Peroxiredoxin 4	3	52	Antioxidant	-
Cu/Zn Superoxide Dismutase	4	57	Antioxidant	+
Calreticulin	5	180	Chaperone	+
B-Actin	6	72	Cytoskeleton	+
Annexin-2	7	87	Vesicle Trafficking	+
Hypothetical	8	167	?	+

disulfide was shown to have increased DSBF. The other 4 proteins that were identified (Table 1 and Figure 2 D, spots 5-7) have various intracellular roles such as chaperone function, cytoskeletal function and vesicular trafficking.

3.4 Verification of mHtt^{103Q} induced Prx-1 diminishment

Prx-1 is one of the three most abundant intracellular proteins within mammalian cells and is of extreme importance guarding the cell against oxidative stress (B. N. Tripathi, et al. 2009). Prx-1 also exhibited the most robust change in DSBF following 2D Redox PAGE analysis (Figure 2D). Thus, we chose to focus on verifying the mHtt^{103Q}

soluble protein lysates were treated in both dimensions with the reducing agent DTT. As expected, a clear diagonal line was revealed with no spots in the off-diagonal zones (Figure 3, A). Also, as a positive control, extracts from cells were exposed to H₂O₂ revealed a moderate increase in disulfide bonded species following Redox 2D-PAGE analysis (Figure 3, B).

3.3 Identification of proteins that undergo changes in DSBF specific to mHtt expression.

Protein spots that exhibited reproducible migration following 2D Redox PAGE were excised, in-gel digested with trypsin and identified by matrix-assisted laser desorption/ionization time-of-flight (MALDI-TOF). Analysis of the protein spots revealed that half of the proteins identified (Table 1 and Figure 2. D, spots 1-4) can be categorized as antioxidant defense proteins. Specifically in the Peroxiredoxin (Prx) family of antioxidant proteins Prx 1, 2 and 4 were identified as the protein species that showed diminished DSBF specific to mHtt^{103Q} expression, whereas the antioxidant Cu/Zn superoxide dismutase was shown to have increased DSBF. The other 4 proteins that were identified (Table 1 and Figure 2 D, spots 5-7) have various intracellular roles such as chaperone function, cytoskeletal function and vesicular trafficking.

3.4 Verification of mHtt^{103Q} induced Prx-1 diminishment

Prx-1 is one of the three most abundant intracellular proteins within mammalian cells and is of extreme importance guarding the cell against oxidative stress (B. N. Tripathi, et al. 2009). Prx-1 also exhibited the most robust change in DSBF following 2D Redox PAGE analysis (Figure 2D). Thus, we chose to focus on verifying the mHtt^{103Q}

specific diminishment of Prx-1 using 1D immunoblot analysis under nonreducing and reducing conditions. At low concentrations of hydrogen peroxide (H_2O_2), Prx-1 exists most commonly in the cell as a disulfide linked homodimer. During catalysis the homodimeric form of Prx-1 can be recycled back to its monomeric form via thioredoxin-mediated reduction.* Nonreduced immunoblot analysis of the soluble protein fraction after 1, 2 and 3 days revealed a mHtt^{103Q} specific decrease in the homodimeric form of Prx-1 at the 2 and 3 day time-points (Figure 4, A). It is important to note that it is the homodimeric form of Prx-1 that is visualized as spot 1 on the 2D Redox PAGE (Figure 2, D). Also apparent under nonreduced conditions a potentially over-oxidized form of Prx 1 is apparent (Figure 4, A indicated by asterisk). Subsequent immunoblot analysis under reduced conditions also revealed a decrease in the monomeric form of Prx-1 at the 2 and 3 day time-points specific to mHtt^{103Q} expression (Figure 4, B). As controls for transgene expression and loading, blots were also probed with anti-GFP and anti-actin antibodies (Figure 4 C, D) which showed progressive induction of GFP-tagged mHtt and equal loading of protein samples respectively. These findings indicate that mHtt expression can provoke overoxidation and loss of Prx1.

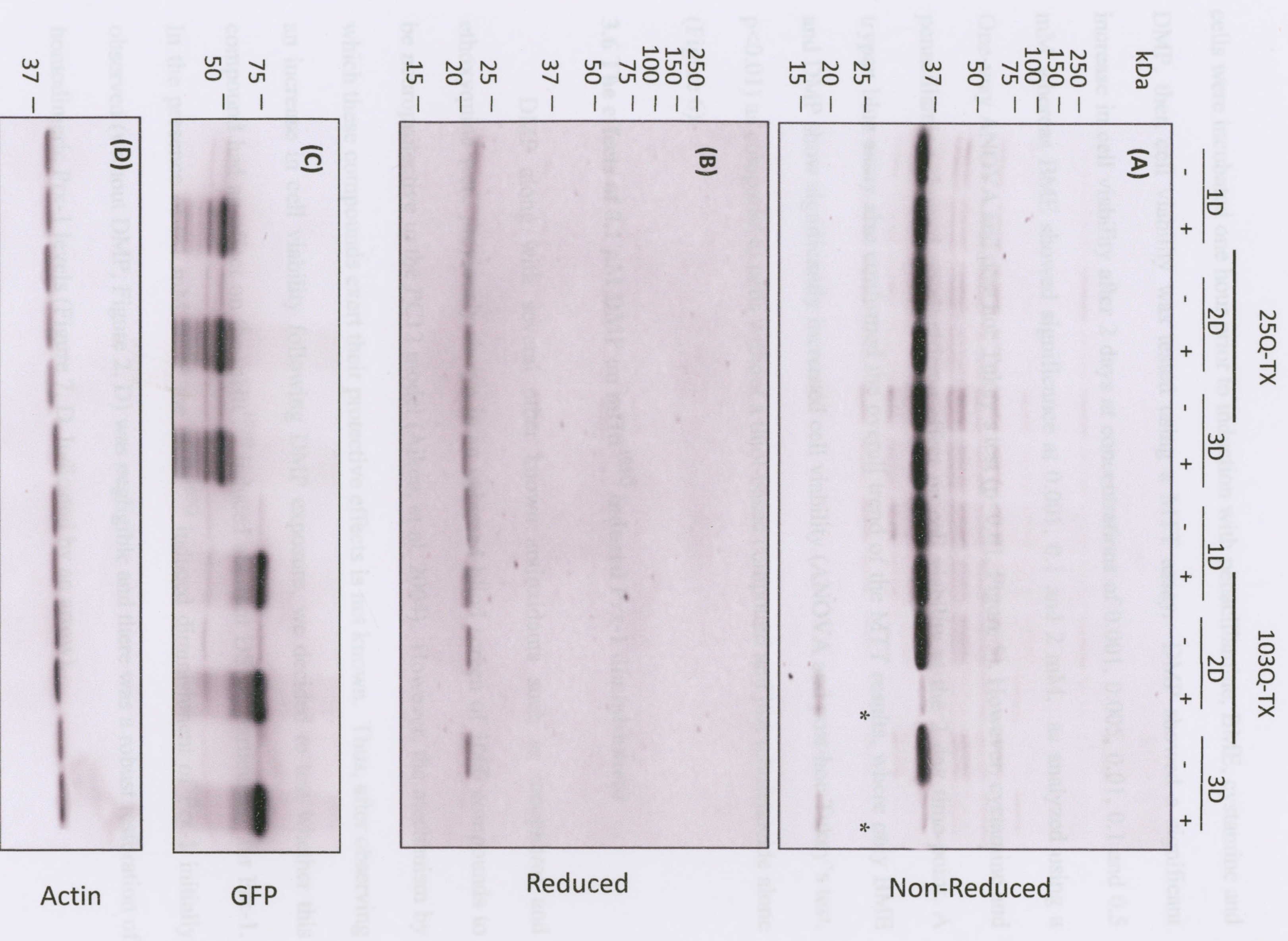
3.5 The effects of thiol-based compounds on PC12 Cell Viability after mHtt^{103Q} induction

Several studies have indicated that antioxidants can counter mHtt-induced toxicity in several cell and animal models however thiol-based compounds have not been extensively tested in the PC12-103Q model. In order to analyze if the neuronal toxicity observed upon mHtt^{103Q} induction could be countered using the thiol-based compounds,

* For information on the catalytic cycle of Prx-1 refer to Appendix, Supplementary Figure 3.

Figure 4.

Timecourse analysis of disulfide bond formation of Peroxiredoxin-1 through one-dimensional nonreducing and reducing SDS-PAGE followed by immunoblotting. PC12 expression of Htt^{25Q} or mHtt^{103Q} was either non-induced (-) or induced (+) over one, two or three days (1D, 2D, 3D) with 2.5 μ M tebufenocide (DMSO alone for non-induced) and harvested in Triton-X100. Disulfide bond formation was visualized with rabbit anti-Prx-1 primary antibody by comparing nonreduced (A) and reduced (B) conditions (N=3). Asterisks denote a potentially overoxidized form of Prx-1. The absence of GFP expression can be seen under uninduced conditions, whereas increasing GFP expression is seen for the induced condition from days 1 through 3 under nonreduced conditions (C). As a control, actin shows equal loading for both uninduced/ induced conditions for Htt25Q and mHtt103Q under nonreduced conditions (D).



cells were incubated one hour prior to induction with penacillamine, BME, cystamine and DMP, then cell viability was tested using a MTT assay. DMP showed a significant increase in cell viability after 2 days at concentrations of 0.001, 0.005, 0.01, 0.1 and 0.5 mM whereas BME showed significance at 0.001, 0.1 and 2 mM, as analyzed using a One-way ANOVA and post hoc Tukey's test ($p < 0.01$, Figure 5). However, cystamine and penacillamine showed no significant effect on cell viability at the 2 day time-point. A trypan blue assay also confirmed the overall trend of the MTT results, where only BME and DMP show significantly increased cell viability (ANOVA and post-hoc Tukey's test, $p < 0.01$) as compared to cells without a thiol-based compound and just tebufenocide alone (Figure 6).

3.6 The effects of 0.1 μ M DMP on mHtt^{103Q} induced Prx-1 diminishment

DMP along with several other known antioxidants such as tocopherol and ethoxyquine were previously shown in an unbiased blind screen of 1000 compounds to be neuroprotective in the PC12 model (Aiken, et al. 2004). However, the mechanism by which these compounds exert their protective effects is not known. Thus, after observing an increase in cell viability following DMP exposure, we decided to test whether this compound had an effect on the mHtt^{103Q} induced aberrant DSBF, particularly for Prx-1. In the presence of 0.1 mM DMP the mHtt^{103Q} induced diminishment of Prx-1 initially observed (without DMP, Figure 2, D) was negligible and there was a robust restoration of homodimeric Prx-1 levels (Figure 7, D. Indicated by an arrow).

Figure 5.

Growth of mHtt induced PC12 cells in the presence of various concentrations of penacillamine, BME, cystamine and DMP. PC12 cell viability after induction of mHtt^{103Q} is represented as a percentage of viable non-induced cells in the presence various concentrations of penacillamine, BME, cystamine and DMP ranging from 0.0001-2 mM. Cell viability was measured through reduction of MTT. Several concentrations of DMP and BME significantly increase cell viability as indicated by asterisks (ANOVA, post-hoc Tukey's test $p < 0.01$). (N=3)

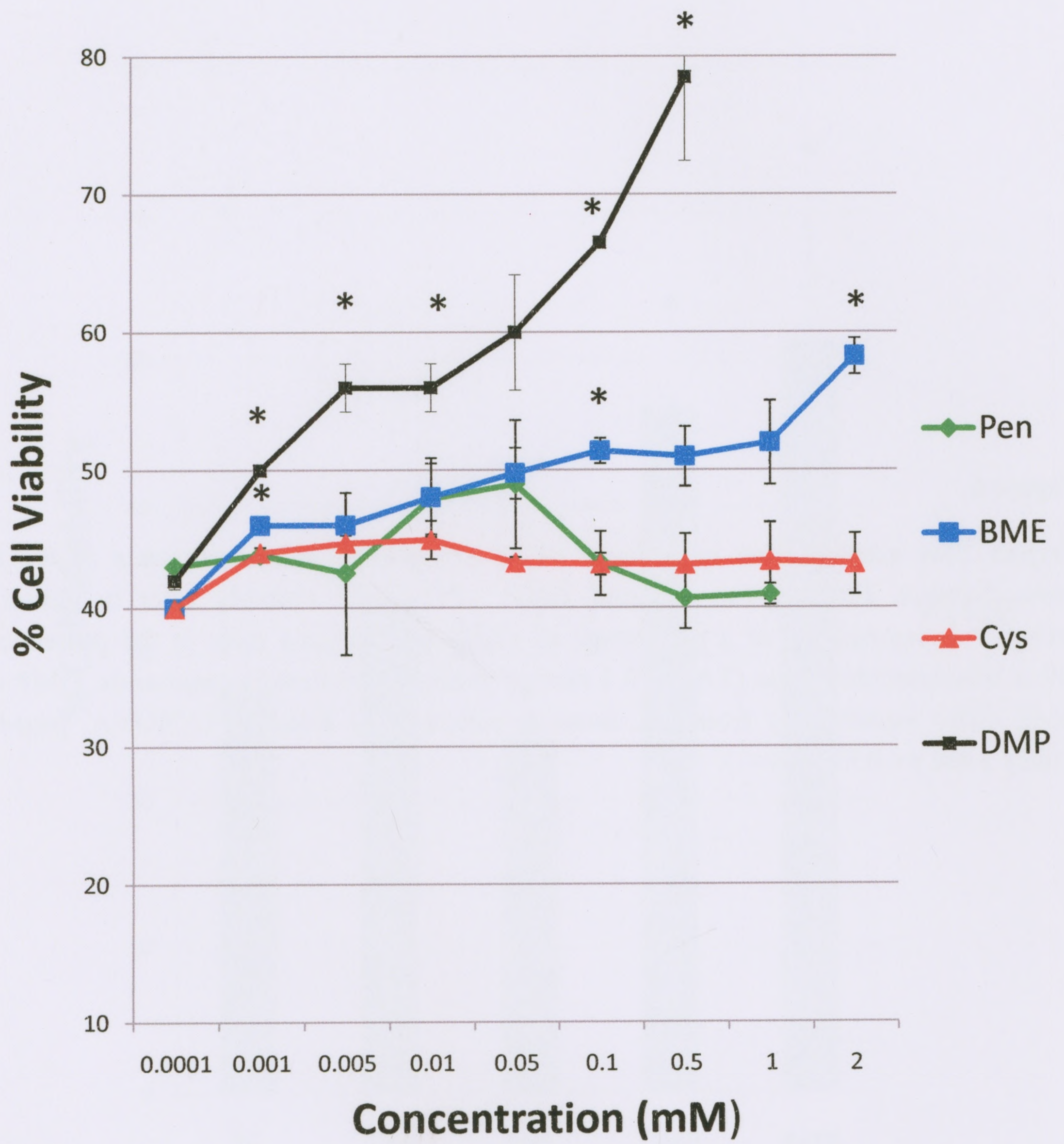


Figure 6.

Trypan Blue confirmation of induced PC12 cell growth in the presence of 0.1 μ M penacillamine, BME, cystamine and DMP. PC12 cell viability after induction of mHtt^{103Q} is represented as a percentage of viable non-induced cells in the presence of either tebufenocid alone (TA) or 0.1 mM of various thiol-based compounds. DMP and BME differ significantly from TA alone as indicated by asterisks (ANOVA, post-hoc Tukey's test $p < 0.01$). (N=3).

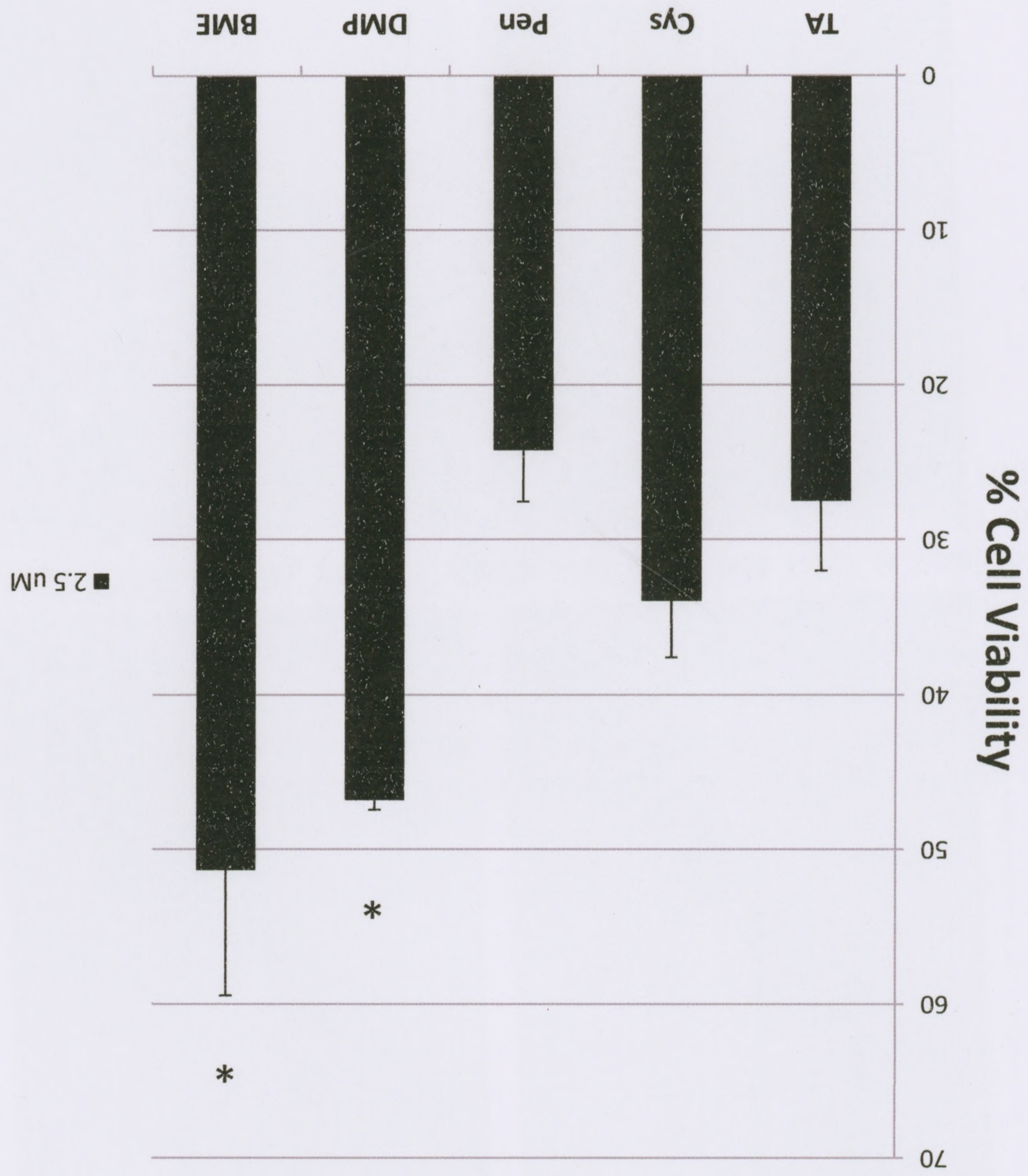
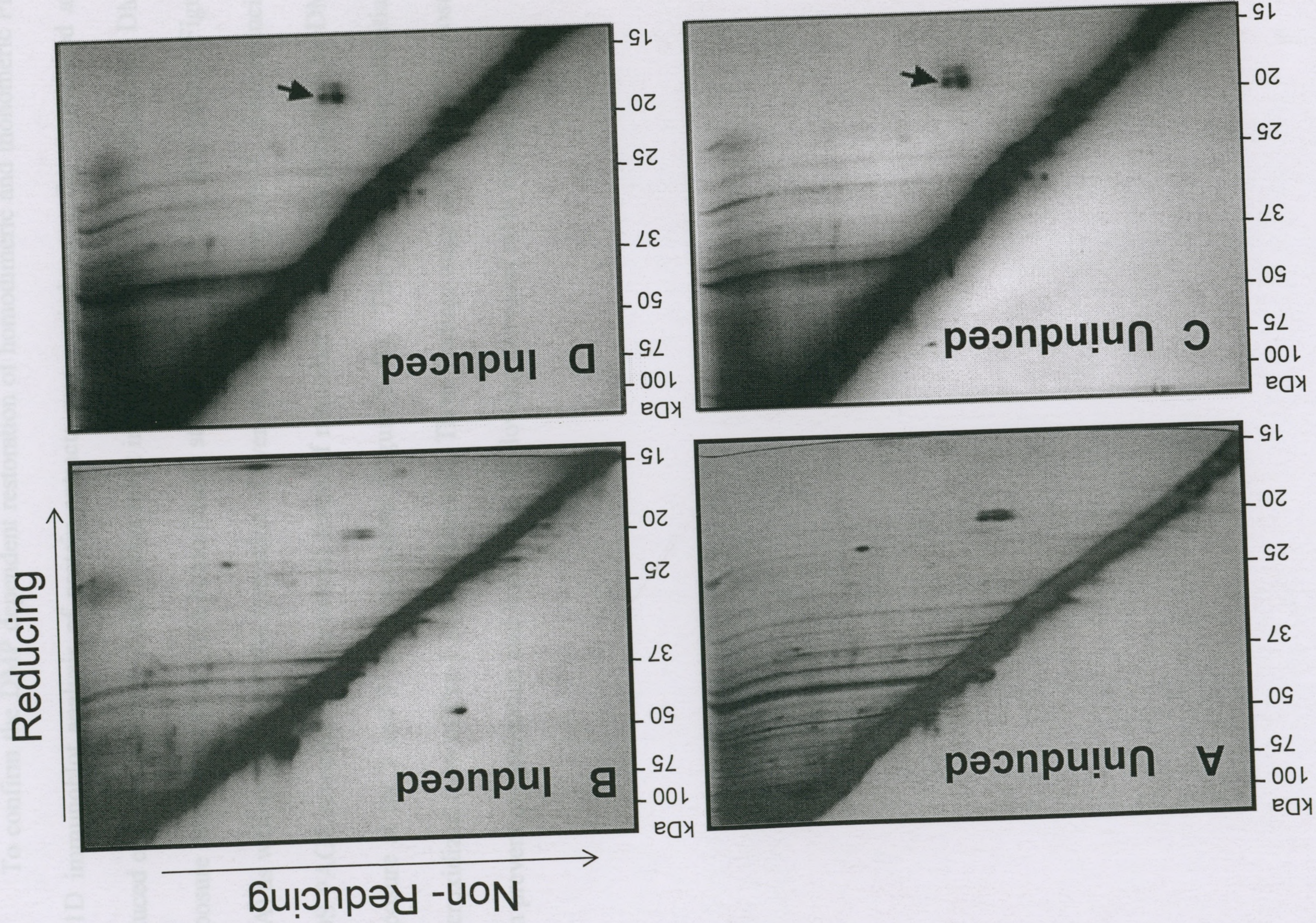


Figure 7.

The effect of 0.1 mM DMP on Prx-1 disulfide bond formation by 2D Redox PAGE. PC12 cells in the presence of 0.1 mM DMP were induced for 2 days with 2.5 μ M tebufenocid. Soluble protein extract were resolved in the first dimension under nonreducing conditions, in the second dimension under reducing conditions and visualized with silver staining. Soluble proteins resolved represent mHtt^{103Q} non-induced (A), mHtt^{103Q} induced (B), mHtt^{103Q} non-induced + 0.1 mM DMP (C) and mHtt^{103Q} induced + 0.1 mM DMP (D). The arrow indicates the DMP specific preservation of homodimeric Prx-1. Non-induced control groups were treated with DMSO a tebufenocid vehicle (A and C). (N=3)



3.7 Verification of the effects of DMP on Prx-1

To confirm the DMP dependent restoration of homodimeric and monomeric Prx-1, 1D immunoblot analysis of protein extracts was carried out under nonreduced and reduced conditions after 1, 2 and 3 days mHtt induction with 2.5 μ M tebufenocide. DMP exposure maintained Prx-1 in a homodimeric state at the 2 and 3 day time-points (Figure 8, A) as well as prevented the formation of over-oxidized forms of Prx-1. Also, reducing SDS-PAGE revealed that the overall levels of monomer Prx-1 were preserved by DMP exposure at the 2 and 3 day time-points (Figure 8, B). The absence of the potentially overoxidized form of Prx-1 is also observed. These findings suggest that DMP exposure can prevent overoxidation and loss of Prx1 following increased mHtt expression.

Figure 8.

Timecourse analysis of Peroxiredoxin-1 disulfide bond formation in the presence of 0.1 μ M DMP with one-dimensional nonreducing and reducing SDS-PAGE followed by immunoblotting. PC12 expression of Htt^{25Q} or mHtt^{103Q} in the presence of 0.1 μ M was either non-induced (-) or induced (+) over one, two or three days (1D, 2D, 3D) with 2.5 μ M tebufenocid (DMSO alone for non-induced) and harvested in Triton-X100. Disulfide bond formation was visualized with rabbit anti-Prx-1 primary antibody by comparing nonreduced (A) and reduced (B) conditions (N=3). Notice the absence of the potentially over-oxidized form of Prx-1. The absence of GFP expression can be seen under uninduced conditions, whereas increasing GFP expression is seen for the induced condition from days 1 through 3 under nonreduced conditions (C). As a control, actin shows equal loading for both uninduced/ induced conditions for Htt^{25Q} and mHtt^{103Q} under nonreduced conditions (D).

25Q-TX

103Q-TX

kDa

1D + - + - + - + - + - +
1D 2D 3D 1D 2D 3D

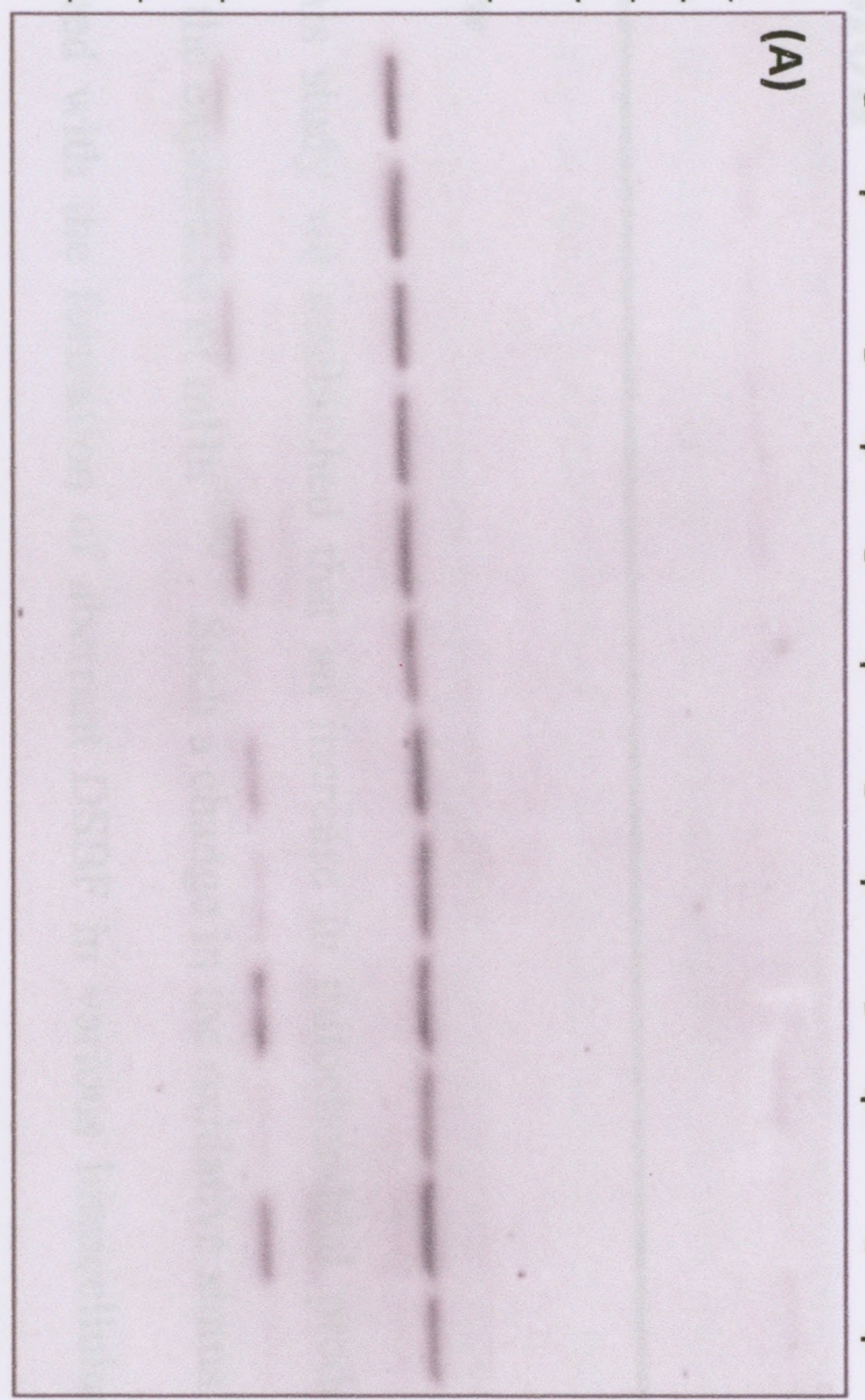
250 -
150 -

75 -

50 -

37 -

25 -
20 -
15 -



Non-Reduced

250 -

100 -

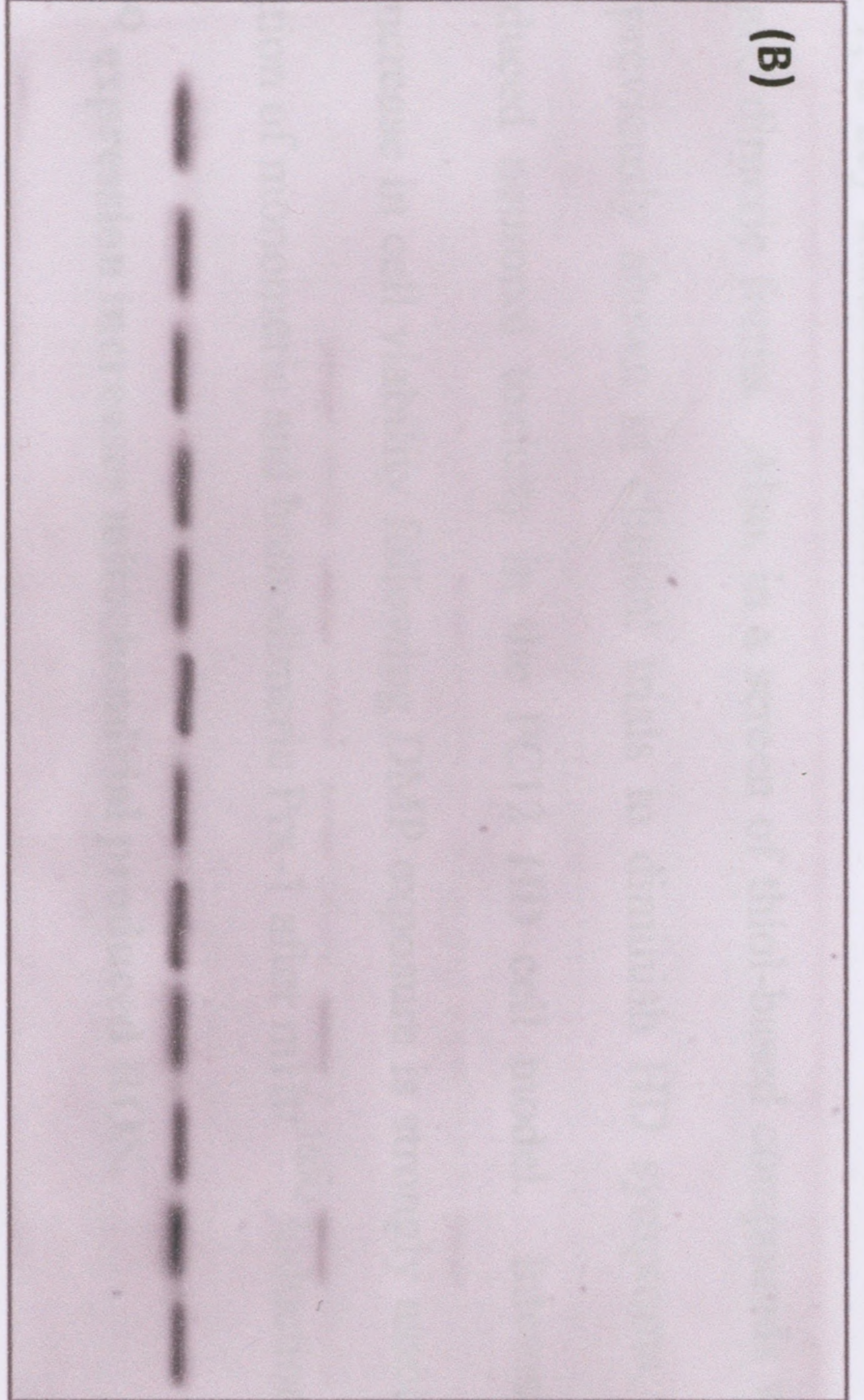
50 -

37 -

25 -

20 -

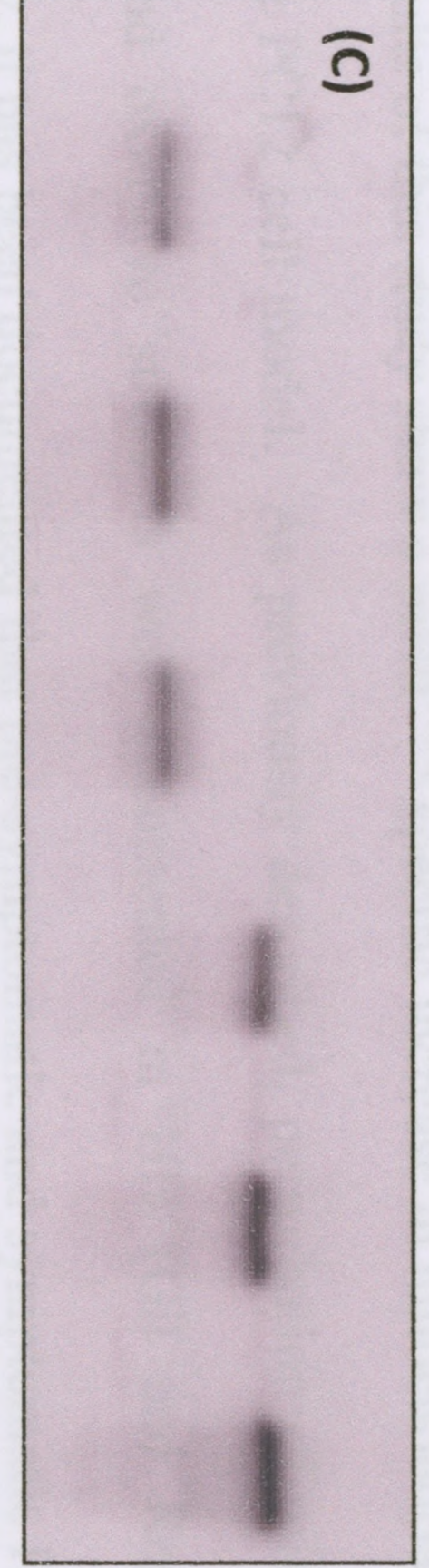
15 -



Reduced

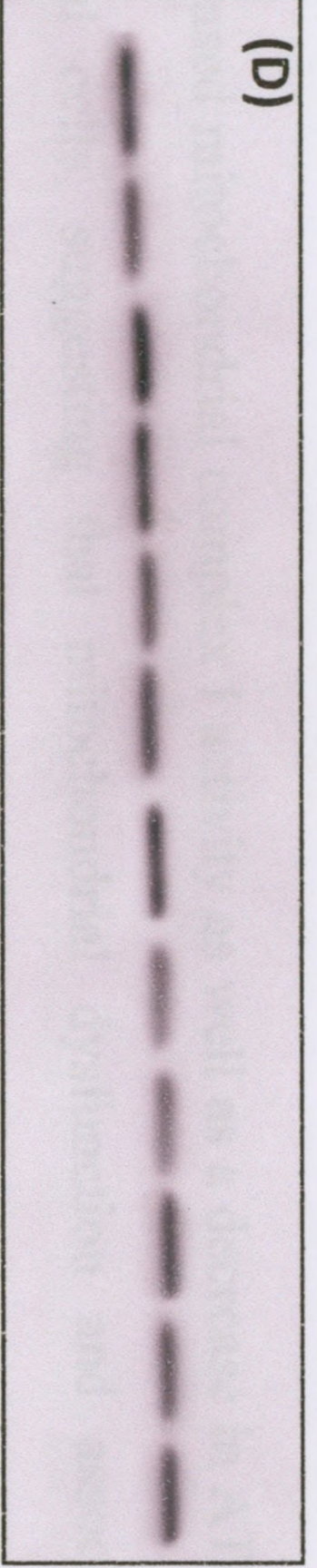
75 -

50 -



GFP

37 -



Actin

Chapter 4

Discussion

4.1 Overview

In this study we established that an increase in mitochondrial produced ROS occurs with the expression of mHtt^{103Q}. Such a change in the oxidative status of the cell also correlated with the formation of aberrant DSBF in various intracellular proteins, such as Prx-1; a key intracellular antioxidant which showed diminishment of both its monomeric and dimeric forms. Also, in a screen of thiol-based compounds we showed that DMP, previously shown in clinical trials to diminish HD symptoms, attenuates mHtt^{103Q} induced neuronal toxicity in the PC12 HD cell model. Interestingly, the significant increase in cell viability following DMP exposure is strongly associated with the preservation of monomeric and homodimeric Prx-1 after mHtt^{103Q} induction.

4.2 mHtt^{103Q} expression increases mitochondrial produced ROS.

Results of this study show a mHtt^{103Q} specific increase in mitochondrial produced ROS in the PC12 cell model. As previously described, perturbation of mitochondrial function and oxidative stress is well documented in HD (Gil and Rego. 2008). Specifically, it has been documented that pre-symptomatic and symptomatic HD patients show decreased mitochondrial complex I activity as well as a decrease in ATP synthesis in neuronal cells, suggesting that mitochondrial dysfunction and associated ROS production plays a role in disease progression (Lodi, et al. 2000). Similarly, oxidative

damage to mitochondrial DNA (mtDNA) can be found in the parietal cortex, while it is absent from regions that do not exhibit neurodegeneration such as the cerebellum (Polidori, et al. 1999). Thus, oxidative stress and mitochondrial perturbation have long been implicated as early modulators of HD neuronal toxicity. In this study, mHtt^{103Q} induction at the 2 day time-point resulted in a dramatic increase in mitochondrial produced ROS suggesting that mitochondria plays a large role in the oxidative stress observed in this cell culture model. However, the numerous cellular effects of mHtt expression leaves unresolved the issue of whether the increase in mitochondrial produced ROS is a primary consequence of perturbed ETC components, a secondary effect of a perturbed ROS detoxification system, or perhaps even a combination of both.

4.3 A mHtt^{103Q} induced increase in mitochondrial ROS production is correlated with aberrant DSBF of key intracellular antioxidant proteins.

Mechanistically, how mHtt induced oxidative stress and the broad spectrum of HD cellular malfunctions arise, remains unknown. For the first time in a HD context, we did a broad screen, using 2D Redox PAGE, of soluble proteins that undergo changes in DSBF specific to mHtt^{103Q} expression. Interestingly in the HD PC12 cell model, the aberrant DSBF of several antioxidant proteins including peroxiredoxins (Prx-1, 2 and 4) as well as cytosolic superoxide dismutase (SOD1) implicate DSBF as a possible mechanism through which oxidative stress and resulting cellular damage may lead to perturbed protein function and downstream neuronal toxicity seen in HD.

The family of peroxiredoxins (Prxs) are one of the most abundant proteins in mammalian cells and play an extremely important role in protecting the cell against oxidative damage (Wood, et al. 2003). Prxs are located in all cells of the body, but are

particularly plentiful in cells susceptible to oxidative stress such as those found in the central nervous system (Wood, et al. 2003). Prxs exist as several isoforms (Prx-1 through -6) exhibiting various subcellular compartmentalization, with specificity dependent on the isoform (Wood, et al. 2003). Specifically, Prx-1 is the most abundant of the Prxs and is found primarily in cytosol and to a small extent in the mitochondria (Gertz et al, 2009). Also, because of their abundance and broad specificity, peroxiredoxins can degrade peroxides and work in concert with other ROS detoxifying enzymes such as SODs and catalase, to detoxify H_2O_2 within the cell (Gertz et al, 2009). Thus, the aberrant DSBF of Prx-1 (loss of the homodimer) and SOD1 (induction of DSBF) may compromise the ROS detoxifying capabilities within the cell.

Through 1D immunoblot analysis of Prx-1, the absence of homodimeric and monomeric Prx-1 following mHtt^{103Q} expression not only confirmed our 2D results but showed a potentially overoxidized form of the Prx-1 homodimer. Overoxidation of Prx-1 occurs in the presence of high levels of peroxides when the peroxidatic cysteine residue (active cysteine) undergoes further oxidation from a sulfenic to a sulfonic acid (Chevallet, et al. 2003). Overoxidation would not only make Prx-1 susceptible to degradation but it would also prevent catalytic recycling of Prx-1 thereby eliminating the antioxidant function of this protein within the cell (Chevallet, et al. 2003).

While DSBF may be part of the normal catalytic function of proteins such as Prx-1, recycling or regeneration of the monomeric form is also essential for maintaining its function. Without proper recycling of Prx-1 via thioredoxin or its overoxidation following high levels of H_2O_2 exposure, the oxidative stress situation that initially occurs in HD neurons may be exacerbated. Recently, Prx-1 and Prx-2 were found to be the most

susceptible of the Prx family to oxidative stress (Cox, et al. 2009). Prx-1 and Prx-2 were found to be susceptible to overoxidation at lower concentrations of H₂O₂ than Prx-3 (Cox, et al. 2009). Interestingly, we did not find aberrant DSBF of Prx-3 with our 2D analysis suggesting that oxidative stress occurring at the 2 day, 2.5 μM induction time-point results in specificity of Prx oxidation. These findings imply an early and important role for Prx-1 oxidation in HD disease progression.

While, Prx-1 is essential in ROS detoxification it has also been shown to regulate the function of several signaling proteins involved in apoptosis (Gertz, et al. 2009). Prx-1 has been shown to bind and inhibit the function of apoptosis signaling kinase factor 1 (ASK1) as well as inhibit p66Shc mediated production of H₂O₂ which acts as a signal to initiate apoptosis (Gertz, et al. 2009). Thus, aberrant DSBF or inactivation by overoxidation of Prx-1 may not only compromise the major ROS detoxifying system of the cell, but potentially initiate early apoptosis through inhibition of p66Shc repression, thereby leading to downstream neuronal toxicity. Thus, finding a way to preserve Prx-1 structure, inhibit aberrant DSBF and maintain the functionality of Prx-1 and antioxidant proteins alike may be essential to preventing HD neuronal toxicity.

Discerning ways to alleviate oxidative stress and determining the importance of antioxidant proteins in disease progression and oxidative resistance has been a focus of HD and neurodegenerative disease research. While several studies have shown the attenuation of HD neuronal toxicity with compounds such as CoQ10, mechanistically how they increase cell viability is unknown. The importance of maintaining the function of various antioxidant proteins in neurodegenerative disorders is well documented for SOD1, glutathione peroxidase and catalase (Chen, et al. 2007, Sorolla, et al. 2008).

Over-expression of the free radical scavenger SOD1 was shown to reverse oxidative stress induced proteasome malfunction, aggregation and cell death observed in HD (Goswami, et al. 2006). Also an early study on Alzheimer's disease, a neurodegenerative disorder associated with oxidative stress, showed elevated mRNA levels of glutathione peroxidase and catalase in amyloid-beta-resistant PC12 clones; further highlighting the importance of antioxidant proteins in preventing neuronal toxicity (Sagara, et al. 1996). In recent years the importance of Prx-1 in Alzheimer's disease has also received much attention as amyloid-beta-resistant PC12 cells showed increased levels of Prx-1 and thioredoxin (Cumming, et al. 2007). Even analysis of cancerous tumors in human breast and lung tissue has shown the preferential induction and elevation of Prx-1 and Trx-1 (Cha, et al. 2009). Thus, antioxidants play an important role in immortalization of tumors and their resistance to apoptosis suggesting Prx-1 may be of extreme importance in protecting cells including neurons from death. These previous studies taken in concert with our observations indicate that preservation of Prx-1 function is a key element in promoting extended cell viability in neurodegenerative diseases such as HD.

4.4 DMP and BME increase cell viability in the PC12 Cell Model.

The thiol-based compounds cystamine, penacillamine, BME and DMP were tested to elucidate their effect on PC12 cell viability. Thiol-based compounds have been extensively studied in terms of neuroprotection, however the observed increases in cell viability in our study appear to be compound specific and mechanistically how protection occurs remains unknown. Rats and mice exposed to 3-Nitropropionic acid (3-NP), an irreversible inhibitor of mitochondrial complex II, are often used to study oxidative stress induced neurodegeneration. 3-NP treatment of non-human primates produces striatal

lesions and neuropathological features similar to HD and has been shown to induce mitochondrial depolarization and increase cell death in HD striatal cell lines (Beal, et al. 1993). Specifically in a rat model of HD, rats pretreated with the antioxidant NAC prior to injection with 3- NP showed significant neuroprotection and decreased oxidative damage in the striatum and cortex (Fontaine, et al. 2000). Similarly, pretreatment of knock-in HD mice with cystamine completely prevented 3-NP mediated cellular toxicity (Mao, et al. 2006). Cystamine has also been previously implicated in other studies as working through inhibition of transglutaminases or caspases. As a result of cystamine's structure we proposed that after metabolism the observed protection may actually work through a thiol-based antioxidant mechanism. However, no significant increase in cell viability was observed with pretreatment of cystamine prior to mHtt^{103Q} induction in our cell model. The lack of neuroprotection in the PC12 HD cell model with cystamine, indicates that cystamine may not have antioxidant effects and suggests that inhibition of transglutaminases or caspases alone is not sufficient for neuroprotection. These findings provide further support that the maintenance of essential antioxidant defense mechanisms within the cell are an integral part of treating neurodegenerative diseases such as HD.

Interestingly, pretreatment of cells with DMP increases cell viability. The significant increase in cell viability observed with DMP treatment is in agreement with a previous study in which an unbiased screen of 1004 compounds in the HD PC12 cell model identified DMP as one of 12 robustly protective compounds (Aiken, et al. 2004). Our study for the first time shows that neuroprotection with DMP is also maintained at an even higher 2.5 μ M tebufenocid induction as compared to 1 mM used in the previous study by Aiken et al., 2004. Until its unbiased identification several years ago, DMP has

not been investigated in a HD context since the 1950s when it was shown in a clinical trial to reduce pathophysiological HD symptoms and halt disease progression in a two-patient study (Nielsen and Butt, 1955). Early studies have also implicated DMP as a metal chelator, but its efficacy in treating Wilson's disease or mercury poisoning have been largely unsuccessful. However, DMP has shown potential in a neurodegenerative mouse model of Parkinson's disease (Oishi, et al. 1993). 1-Methyl-4-phenyl-1,2,3,6-tetrahydropyridine (MPTP) produces Parkinson's in humans and selective degeneration of nigrostriatal dopaminergic neurons in primates and mice by inhibiting complex 1 of the mitochondria and enhancing superoxide generation (Oishi, et al. 1993). Interestingly, pretreatment with DMP showed inhibition of MPTP induced neurodegeneration in mice and increased GSH levels (Oishi, et al. 1993). Therefore, the DMP mediated increase in cell viability seen in our HD PC12 cell model may be the result of the thiol-based protection of essential antioxidant proteins such as GSH or perhaps Prx-1, and acts by maintaining these molecules in a reduced state. Also, the significant increase in cell viability with the crude thiol-based reducing agent BME further suggests that reduction of aberrant DSBF may be an integral part of maintaining neuronal viability in an HD context. Importantly, the absence of a significant effect of the metal chelator penicillamine on cell viability in our HD PC12 cell model suggests the neuroprotection observed with DMP is not occurring through metal chelation.

4.5 DMP preserves the homodimeric and monomeric forms of Prx-1.

As a result of DMP's significant increase in cell viability and previous use in clinical trials we chose to focus on the effect of 0.1 mM DMP on DSBF of Prx-1. The DMP specific preservation of homodimeric and monomeric Prx-1 as seen with 2D

analysis and 1D immunoblotting, is correlated with increased cell viability seen at 0.1 mM DMP exposure. These findings suggest that DMP may work to protect neuronal cell death in HD through the thiol-based preservation of Prx-1 and potentially related proteins such as thioredoxin. Also, the preservation of Prx-1 and increase in cell viability seen with 0.1 mM DMP provides further support that Prx-1 is an extremely important protein that when functionally inactivated may contribute to HD neuronal toxicity and disease progression. Also, for the first time this study provides a mechanism through which loss of antioxidant protein function may contribute to cellular perturbations associated with HD. While perturbations of Prx-1 function have up until now been largely uninvestigated in a HD context a recent study showed how Prx-1 knockdown in HeLa cells leads to apoptosis (S. Y. Kim, et al. 2008). Prx-1 has been shown to negatively regulate ASK-1, with knockdown of Prx-1 leading to activation of ASK1 and the downstream effectors p38 and JNK resulting in cell death (Kim, et al. 2008). It is reasonable to propose that aberrant DSBF or overoxidation of Prx-1 results in an increase of not only oxidative stress, but also the premature activation of the apoptotic pathway; both contributing in tandem to the neuronal toxicity seen in HD.

4.6 Conclusions and Future Direction

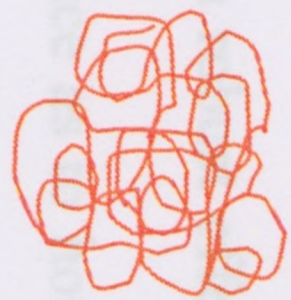
For the first time in a HD context, a dramatic increase in mitochondrial produced ROS was correlated with aberrant DSBF in antioxidant proteins. This study implicates DSBF as a possible mechanism through which oxidative stress may contribute to the characteristic neuronal toxicity of HD. While the initial trigger for oxidative stress in HD is poorly defined, being able to prevent the resulting oxidative modifications to biological macromolecules may be a possible area to focus future therapeutic treatment. In

summary, our results show that maintaining the functional integrity of key antioxidant proteins such as Prx-1 can have a valuable effect on cell viability and thus provides further support that oxidative stress and compromised oxidant defense mechanisms do play an essential role in HD disease progression (Figure 9). While, DSBF and the subsequent overoxidation of Prx-1 would result in compromised ROS detoxification abilities it may also cause perturbation of other cellular functions as a result of Prx-1's multifaceted function within the cell. While Prx-1 has been shown to play an important role in apoptosis it also possesses a chaperone function. Thus, inactivation of Prx-1 may cause increased oxidative stress, early apoptosis and contribute to aggregate formation seen in HD via perturbed chaperone function. Future studies should analyze the functionality of wildtype Prx-1 and its catalytically inactive cysteine mutant with overexpression studies to see if rescue of the HD phenotype is dependent on the antioxidant activity of Prx1. Also, to better understand Prx-1's role in aggregate induced toxicity an epitope tagged version of Prx-1 coupled with immunofluorescent microscopy

Figure 9.

Proposed model of mHtt-mediated effects on protein disulfide bond formation.

Accumulation of mHtt is believed to perturb mitochondrial function leading to increased electron leakage and ROS production. Increased mHtt expression may also lead to either decreased expression or post-translational modifications of antioxidant protein. Ultimately, increased ROS production will promote the formation of aberrant protein disulfide bonds leading to changed in the normal function of the affected protein (ie. cellular metabolism and signaling). DSBF may also promote protein misfolding and the accumulation of toxic aggregates. Treatment of cells with thiol-based antioxidants may either directly reduce disulfide bonds or indirectly lead to ROS detoxification by increasing the intracellular levels of glutathione, an essential cofactor for glutathione peroxidase. The reduction of aberrant protein disulfide bonds by thiol-antioxidants may restore normal protein function and/or decrease protein aggregation leading to increased cell survival.



mHtt expression



Perturbed mitochondrial function

Increased ROS production



Thiol-antioxidant drugs

?



-Altered signaling /metabolism

-Increased protein aggregation



would be beneficial to see whether there is co-localization of Prx-1 with HD aggregates. Also, 2D Redox PAGE followed by MALDI-TOF of the insoluble protein fraction would help elucidate whether proteins such as Prx-1 are shifting from an soluble state to an insoluble aggregate form analysis upon induction of mHtt.

While several studies have shown increased cell viability in various neurodegenerative disease models with antioxidant treatment, this study for the first time provides a mechanistic understanding of how this may occur. Attenuation of the HD phenotype in the PC12 cell model was observed with DMP pretreatment prior to mHtt^{103Q} induction. Through 2D Redox PAGE and 1D immunoblot analysis our results suggest DMP increases cell viability through preservation of Prx-1 function. Mechanistically preservation may occur through reduction of the Prx-1 homodimer and/or the reduction of thioredoxin; both of which would act to preserve the catalytic function of Prx-1. Similarly, DMP may have effects on increasing GSH levels within the cell, as seen in a Parkinson's disease animal model, thus having an indirect effect on Prx-1 preservation. Future studies should focus on elucidating the effects of DMP on Prx-1 related proteins such as thioredoxin as well as GSH. Also, our results implicate DMP or structurally related compounds as possible future therapeutics in HD. DMP appears to have a robust effect on cell viability in our HD Pc12 cell model and provides the first evidence as to how thiol-based antioxidants in a HD context may exert their protective effects. However, the difficulty in administering this compound (by intramuscular injection) in addition to its numerous side effects as reported in HD and Wilson's disease patients suggest DMP may not be an ideal treatment. Thus, a highly related compound such as Meso 2, 3-dimercaptosuccinic acid (DMSA) which is orally active and has fewer

side effects as well as significant neuroprotective capabilities may be a better therapeutic (Pachauri, et al. 2009). However, before testing in humans, 2D Redox analysis in a mouse model of HD such as the R2/6 mouse that over-expresses exon 1 (as in the PC12 model) should be investigated with and without compounds such as DMP or DMSA.

In conclusion, these results provide support of our initial hypothesis that alterations in disulfide-linked proteins may be a mechanism through which oxidative stress and neuronal cell death in HD progresses. Also, thiol-based compounds such as DMP have been shown for the first time to counter these effects through preservation of Prx-1 functional integrity, implicating Prx-1 as a key protein involved in HD progression and revealing a new avenue for therapeutic drug treatments.

BIBLIOGRAPHY

- Aiken CT, Tobin AJ, Schweitzer ES. A cell-based screen for drugs to treat Huntington's disease. *Neurobiol.Dis.* 2004, (3):546-555.
- Beal MF, Brouillet E, Jenkins BG, Ferrante RJ, Kowall NW, Miller JM, et al. Neurochemical and histologic characterization of striatal excitotoxic lesions produced by the mitochondrial toxin 3-nitropropionic acid. *J.Neurosci.* 1993, (10):4181-4192.
- Beal MF, Brouillet E, Jenkins B, Henshaw R, Rosen B, Hyman BT. Age-dependent striatal excitotoxic lesions produced by the endogenous mitochondrial inhibitor malonate. *J.Neurochem.* 1993, 61(3):1147-1150.
- Bennett EJ, Shaler TA, Woodman B, Ryu KY, Zaitseva TS, Becker CH, et al. Global changes to the ubiquitin system in Huntington's disease. *Nature* 2007, 448(7154):704-708.
- Bogdanov MB, Andreassen OA, Dedeoglu A, Ferrante RJ, Beal MF. Increased oxidative damage to DNA in a transgenic mouse model of Huntington's disease. *J.Neurochem.* 2001, 79(6):1246-1249.
- Cha MK, Suh KH, Kim IH. Overexpression of peroxiredoxin I and thioredoxin1 in human breast carcinoma. *J.Exp.Clin.Cancer Res.* 2009 30;28:93.
- Chen CM, Wu YR, Cheng ML, Liu JL, Lee YM, Lee PW, et al. Increased oxidative damage and mitochondrial abnormalities in the peripheral blood of Huntington's disease patients. *Biochem.Biophys.Res.Commun.* 2007, 27;359(2):335-340.
- Chevallet M, Wagner E, Luche S, van Dorsselaer A, Leize-Wagner E, Rabilloud T. Regeneration of peroxiredoxins during recovery after oxidative stress: only some overoxidized peroxiredoxins can be reduced during recovery after oxidative stress. *J.Biol.Chem.* 2003, 26;278(39):37146-37153.
- Cox AG, Pearson AG, Pullar JM, Jonsson TJ, Lowther WT, Winterbourn CC, et al. Mitochondrial peroxiredoxin 3 is more resilient to hyperoxidation than cytoplasmic peroxiredoxins. *Biochem.J.* 2009,12;421(1):51-58.
- Cumming RC, Andon NL, Haynes PA, Park M, Fischer WH, Schubert D. Protein disulfide bond formation in the cytoplasm during oxidative stress. *J.Biol.Chem.* 2004, 21;279(21):21749-21758.
- Cumming RC, Dargusch R, Fischer WH, Schubert D. Increase in expression levels and resistance to sulfhydryl oxidation of peroxiredoxin isoforms in amyloid beta-resistant nerve cells. *J.Biol.Chem.* 2007, 19;282(42):30523-30534.

DiFiglia M, Sapp E, Chase KO, Davies SW, Bates GP, Vonsattel JP, et al. Aggregation of huntingtin in neuronal intranuclear inclusions and dystrophic neurites in brain. *Science* 1997, 26;277(5334):1990-1993.

Ding Q, Keller JN. Proteasomes and proteasome inhibition in the central nervous system. *Free Radic.Biol.Med.* 2001, 1;31(5):574-584.

Dragatsis I, Efstratiadis A, Zeitlin S. Mouse mutant embryos lacking huntingtin are rescued from lethality by wild-type extraembryonic tissues. *Development* 1998, 125(8):1529-1539.

Fontaine MA, Geddes JW, Banks A, Butterfield DA. Effect of exogenous and endogenous antioxidants on 3-nitropropionic acid-induced in vivo oxidative stress and striatal lesions: insights into Huntington's disease. *J.Neurochem.* 2000, 75(4):1709-1715.

Fox JH, Barber DS, Singh B, Zucker B, Swindell MK, Norflus F, et al. Cystamine increases L-cysteine levels in Huntington's disease transgenic mouse brain and in a PC12 model of polyglutamine aggregation. *J.Neurochem.* 2004, 91(2):413-422.

Gertz M, Fischer F, Leipelt M, Wolters D, Steegborn C. Identification of Peroxiredoxin 1 as a novel interaction partner for the lifespan regulator protein p66Shc. *Aging (Albany NY)* 2009, 30;1(2):254-265.

Gil JM, Rego AC. Mechanisms of neurodegeneration in Huntington's disease. *Eur.J.Neurosci.* 2008, 27(11):2803-2820

Goswami A, Dikshit P, Mishra A, Mulherkar S, Nukina N, Jana NR. Oxidative stress promotes mutant huntingtin aggregation and mutant huntingtin-dependent cell death by mimicking proteasomal malfunction. *Biochem.Biophys.Res.Commun.* 2006, 31;342(1):184-190.

Gu M, Gash MT, Mann VM, Javoy-Agid F, Cooper JM, Schapira AH. Mitochondrial defect in Huntington's disease caudate nucleus. *Ann.Neurol.* 1996, 39(3):385-389.

Gutekunst CA, Li SH, Yi H, Ferrante RJ, Li XJ, Hersch SM. The cellular and subcellular localization of huntingtin-associated protein 1 (HAP1): comparison with huntingtin in rat and human. *J.Neurosci.* 1998, 1;18(19):7674-7686.

Hoffner G, Soues S, Djian P. Aggregation of expanded huntingtin in the brains of patients with Huntington disease. *Prion* 2007, 1(1):26-31.

Jenkins JB, Conneally PM. The Paradigm of Huntington's Disease. *Am. J. Hum. Gent.* 1989, 45: 169-175.

Kahlem P, Green H, Djian P. Transglutaminase action imitates Huntington's disease: selective polymerization of Huntingtin containing expanded polyglutamine. *Mol.Cell* 1998, 1(4):595-601.

Kalinina EV, Chernov NN, Saprin AN. Involvement of thio-, peroxi-, and glutaredoxins in cellular redox-dependent processes. *Biochemistry (Mosc)* 2008, 73(13):1493-1510.

Karpuj MV, Becher MW, Springer JE, Chabas D, Youssef S, Pedotti R, et al. Prolonged survival and decreased abnormal movements in transgenic model of Huntington disease, with administration of the transglutaminase inhibitor cystamine. *Nat.Med.* 2002, 8(2):143-149.

Kim SY, Kim TJ, Lee KY. A novel function of peroxiredoxin 1 (Prx-1) in apoptosis signal-regulating kinase 1 (ASK1)-mediated signaling pathway. *FEBS Lett.* 2008, 11;582(13):1913-1918.

Kim YJ, Yi Y, Sapp E, Wang Y, Cuiffo B, Kegel KB, et al. Caspase 3-cleaved N-terminal fragments of wild-type and mutant huntingtin are present in normal and Huntington's disease brains, associate with membranes, and undergo calpain-dependent proteolysis. *Proc.Natl.Acad.Sci.U.S.A.* 2001, 23;98(22):12784-12789.

Liu H, Nishitoh H, Ichijo H, Kyriakis JM. Activation of apoptosis signal-regulating kinase 1 (ASK1) by tumor necrosis factor receptor-associated factor 2 requires prior dissociation of the ASK1 inhibitor thioredoxin. *Mol.Cell.Biol.* 2000 Mar, (6):2198-2208.

Lodi R, Schapira AH, Manners D, Styles P, Wood NW, Taylor DJ, et al. Abnormal in vivo skeletal muscle energy metabolism in Huntington's disease and dentatorubropallidoluysian atrophy. *Ann.Neurol.* 2000, 48(1):72-76.

Mao Z, Choo YS, Lesort M. Cystamine and cysteamine prevent 3-NP-induced mitochondrial depolarization of Huntington's disease knock-in striatal cells. *Eur.J.Neurosci.* 2006, 23(7):1701-1710.

Nasir J, Floresco SB, O'Kusky JR, Diewert VM, Richman JM, Zeisler J, et al. Targeted disruption of the Huntington's disease gene results in embryonic lethality and behavioral and morphological changes in heterozygotes. *Cell* 1995, 2;81(5):811-823.

Nielson JM, Butt EM. Treatment of Huntington's chorea with bal. *Bull.Los Angel Neuro Soc.* 1955, 20(1):38-39.

Oishi T, Hasegawa E, Murai Y. Sulfhydryl drugs reduce neurotoxicity of 1-methyl-4-phenyl-1,2,3,6-tetrahydropyridine (MPTP) in the mouse. *J.Neural Transm.Park.Dis.Dement.Sect.* 1993, 6(1):45-52.

- Pachauri V, Saxena G, Mehta A, Mishra D, Flora SJ. Combinational chelation therapy abrogates lead-induced neurodegeneration in rats. *Toxicol.Appl.Pharmacol.* 2009, 15;240(2):255-264.
- Polidori MC, Mecocci P, Browne SE, Senin U, Beal MF. Oxidative damage to mitochondrial DNA in Huntington's disease parietal cortex. *Neurosci.Lett.* 1999, 3;272(1):53-56.
- Quintanilla RA, Johnson GV. Role of mitochondrial dysfunction in the pathogenesis of Huntington's disease. *Brain Res.Bull.* 2009, 28;80(4-5):242-247.
- Ratovitski T, Gucek M, Jiang H, Chighladze E, Waldron E, D'Ambola J, et al. Mutant huntingtin N-terminal fragments of specific size mediate aggregation and toxicity in neuronal cells. *J.Biol.Chem.* 2009, 17;284(16):10855-10867.
- Riley BE, Orr HT. Polyglutamine neurodegenerative diseases and regulation of transcription: assembling the puzzle. *Genes Dev.* 2006, 15;20(16):2183-2192.
- Sagara Y, Dargusch R, Klier FG, Schubert D, Behl C. Increased antioxidant enzyme activity in amyloid beta protein-resistant cells. *J.Neurosci.* 1996, 15;16(2):497-505.
- Sayre LM, Perry G, Smith MA. Oxidative stress and neurotoxicity. *Chem.Res.Toxicol.* 2008, 21(1):172-188.
- Schaffar G, Breuer P, Boteva R, Behrends C, Tzvetkov N, Strippel N, et al. Cellular toxicity of polyglutamine expansion proteins: mechanism of transcription factor deactivation. *Mol.Cell* 2004, 2;15(1):95-105.
- Schilling G, Coonfield ML, Ross CA, Borchelt DR. Coenzyme Q10 and remacemide hydrochloride ameliorate motor deficits in a Huntington's disease transgenic mouse model. *Neurosci.Lett.* 2001, 27;315(3):149-153.
- Seong IS, Ivanova E, Lee JM, Choo YS, Fossale E, Anderson M, et al. HD CAG repeat implicates a dominant property of huntingtin in mitochondrial energy metabolism. *Hum.Mol.Genet.* 2005, 1;14(19):2871-2880.
- Sorolla MA, Reverter-Branchat G, Tamarit J, Ferrer I, Ros J, Cabiscol E. Proteomic and oxidative stress analysis in human brain samples of Huntington disease. *Free Radic.Biol.Med.* 2008, 1;45(5):667-678.
- Stack EC, Matson WR, Ferrante RJ. Evidence of oxidant damage in Huntington's disease: translational strategies using antioxidants. *Ann.N.Y.Acad.Sci.* 2008, 1147:79-92.
- St-Pierre J, Drori S, Uldry M, Silvaggi JM, Rhee J, Jager S, et al. Suppression of reactive oxygen species and neurodegeneration by the PGC-1 transcriptional coactivators. *Cell* 2006, 20;127(2):397-408.

Sugars KL, Brown R, Cook LJ, Swartz J, Rubinsztein DC. Decreased cAMP response element-mediated transcription: an early event in exon 1 and full-length cell models of Huntington's disease that contributes to polyglutamine pathogenesis. *J.Biol.Chem.* 2004, 6;279(6):4988-4999.

Sultana R, Butterfield DA. Slot-blot analysis of 3-nitrotyrosine-modified brain proteins. *Methods Enzymol.* 2008, 440:309-316.

Tripathi BN, Bhatt I, Dietz KJ. Peroxiredoxins: a less studied component of hydrogen peroxide detoxification in photosynthetic organisms. *Protoplasma* 2009, 235(1-4):3-15.

Trushina E, McMurray CT. Oxidative stress and mitochondrial dysfunction in neurodegenerative diseases. *Neuroscience* 2007, 14;145(4):1233-1248.

Vonsattel, J.P. , DiFiglia, M. Huntington disease. *J. Neuropathol. Exp. Neurol.* 1998, 57, 369-384.

Wood ZA, Schroder E, Robin Harris J, Poole LB. Structure, mechanism and regulation of peroxiredoxins. *Trends Biochem.Sci.* 2003, 28(1):32-40.

Wytenbach A, Sauvageot O, Carmichael J, Diaz-Latoud C, Arrigo AP, Rubinsztein DC. Heat shock protein 27 prevents cellular polyglutamine toxicity and suppresses the increase of reactive oxygen species caused by huntingtin. *Hum.Mol.Genet.* 2002, 11(9):1137-1151.

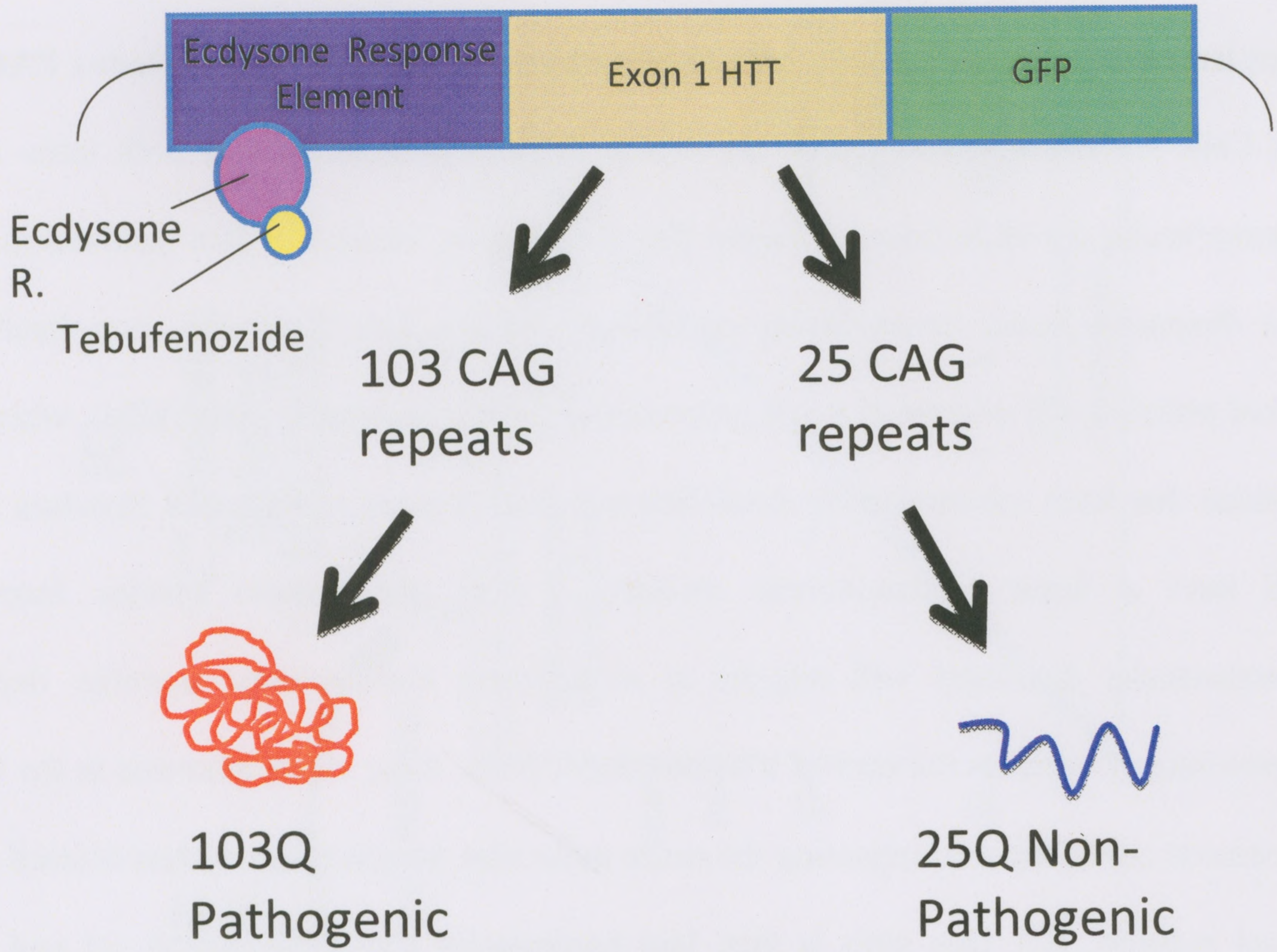
Young AJ, Johnson S, Steffens DC, Doraiswam PM. Coenzyme Q10: a review of its promise as a neuroprotectant. *CNS Spectr.* 2007, 12(1):62-68.

Appendix

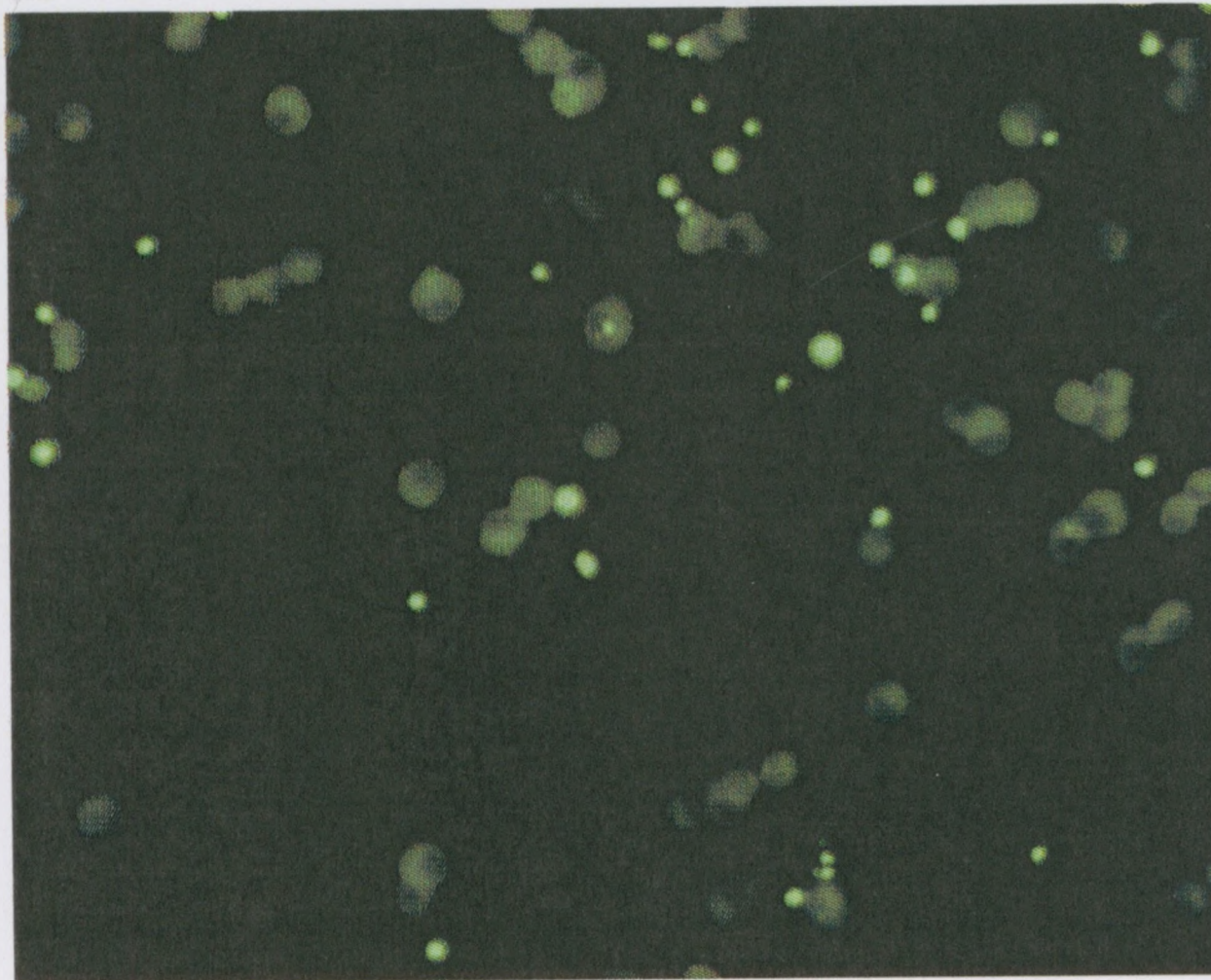
Supplementary Figures

Supplementary Figure 1. HD Cell Model: Transgenic PC12 Cell Line. (A) PC12 cells have been stably transfected with a plasmid containing the exon 1 of the *HTT* gene, with 103 CAG (103Q) repeats or 25 CAG (25Q) repeats and fused to an EGFP marker (C. T. Aiken, et al. 2004). The cell line is consistently maintained at a low passage number. Transcription of the Htt transgene is driven by an ecdysone regulated promoter that can be turned on or off with the addition or removal of the nonsteroidal ecdysone analog tebufenocide. Tebufenocide alone is a sufficient additive to initiate transcription as PC12 cells were also stably transfected with a plasmid containing the ecdysone receptor with a constitutively active promoter. Thus, using two versions of the same cell line (25Q and 103Q), the effects of mHtt expression may be compared at will with wildtype Htt expression. (B.i) PC12 cells exhibit similar characteristics to mature neurons such as neuron-like processes (B.ii.) The EGFP- tagged transgene can also be monitored with fluorescent microscopy to ensure transgene expression and aggregate formation. As previously documented and observed in this study, PC12 cells display rapid (48h) and robust (~50%) cell death upon 2.5 uM tebufenocide induction.

(A)

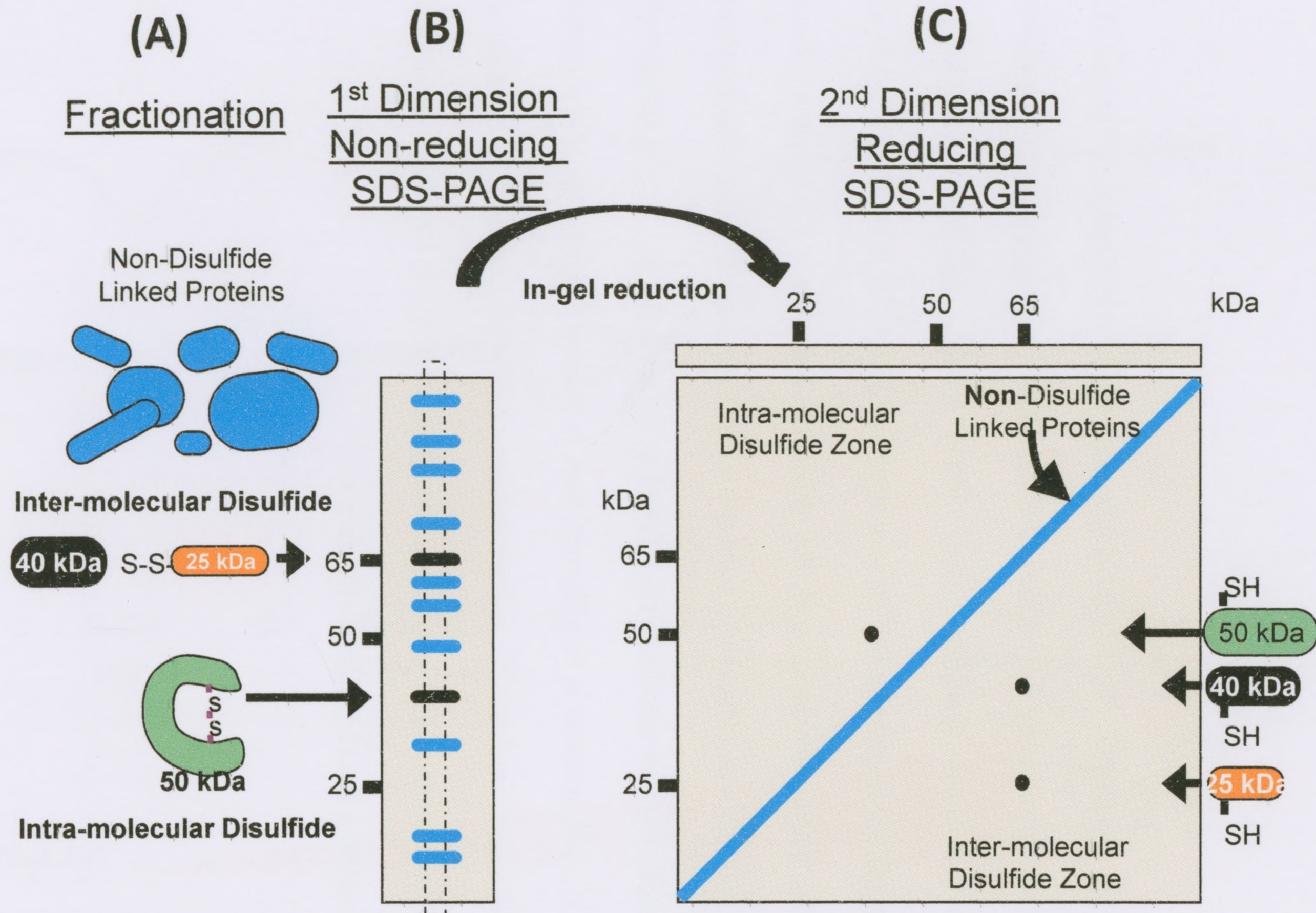


(B)



Supplementary Figure 2. Schematic Explanation of Two-dimensional Redox PAGE.

(A) Cells are fractionated to isolate all soluble non-disulfide as well as both intra- and intermolecular disulfide linked proteins. (B) The protein mixture is then resolved in the first dimension under non-reducing conditions. In the first dimension, non-disulfide linked proteins will migrate at a rate proportional to their molecular mass (kDa), whereas proteins that form intramolecular disulfides will have a more compressed structure and will have a faster electrophoretic mobility. Also, the protein species forming intermolecular disulfides will migrate at an apparent electrophoretic mobility that is approximately equal to the sum of its component parts. After electrophoresis in the first dimension a gel strip encompassing the entire molecular weight range is then excised and in-gel reduced. (C) This strip is then laid horizontally against a second gel and the proteins are resolved under reduced conditions in the second dimension. The resultant resolved protein that contain no disulfide bonds will appear on a diagonal line across the 2D-gel, whereas proteins that form disulfide bond will appear in the off - diagonal zones as distinct spots. Specifically, proteins that form intramolecular disulfide will appear to the left and above the diagonal line, whereas those that form intermolecular disulfides will appear to the right and below.



Supplementary Figure 3. Prx-1 Structure and Catalytic Function Under Oxidative

Stress. Peroxiredoxin exerts its protective antioxidant role by essentially sacrificing itself and forming a catalytic disulfide bond. Prx-1 reduces and detoxifies H_2O_2 to their corresponding alcohols and water. At low levels of ROS, Prx-1 contains two cysteines in its active site, the peroxidatic and the reducing cysteine. Upon detoxification the peroxidatic cysteine is oxidized to a sulfenic acid (a reversible state) which subsequently attacks the sulfhydryl on another Prx-1 forming a homodimer. At physiologically basal levels of H_2O_2 , this process is readily reversed through reduction of the homodimeric disulfide bond by thioredoxin an oxoreductase. However, with an increasing oxidative insult, irreversible overoxidation of the peroxidatic cysteine to sulfinic and sulfonic acids can occur, rendering Prx-1 functionally inactive.

